J. Mech. Phys. Solids 215 (2026) 106740

Contents lists available at ScienceDirect

Journal of the Mechanics and Physics of Solids

journal homepage: www.elsevier.com/locate/jmps

Fractional calculus based elasticity obtained from homogenization

Kshiteej J. Deshmukh [a], Liping Liu [b,c], Pradeep Sharma [a,d,e,*]

[a] Department of Mechanical and Aerospace Engineering, University of Houston, TX, 77204, USA
[b] Department of Mechanical and Aerospace Engineering, Rutgers University, NJ, 08854, USA
[c] Department of Mathematics, Rutgers University, NJ, 08854, USA
[d] Department of Physics, University of Houston, TX, 77204, USA
[e] Materials Science and Engineering Program, University of Houston, TX, 77204, USA

ARTICLE INFO

Keywords:
Fractional calculus
Homogenization
Elasticity

ABSTRACT

Anomalous phenomena, such as diffusion in biological systems, scale-dependent plasticity in thin films, and electromagnetic wave propagation in complex media, often defy explanation by conventional theories rooted in integer-order calculus. Models based on fractional calculus have proven effective in capturing such behaviors, yet the fractional exponents they employ are typically introduced as empirical fitting parameters without grounding in the underlying physics. In this work, we propose that fractional differential equations can emerge naturally through homogenization of materials with complex microstructures, which are themselves the source of the anomalous behavior that necessitates a fractional description. Focusing on linear elasticity, we identify precise microstructural conditions that give rise to emergent fractional behavior. In the static regime, homogenization reveals that the order of the fractional derivative is directly linked to the power-law exponent of the microstructure's autocovariance function. By connecting microscale structural variation to macroscale material response, our study opens new avenues for designing architectured materials with tailored anomalous properties. The implications of this work extend broadly across physics, biology, materials science, and beyond.

1. Introduction

Modeling material behavior and physical systems using fractional derivatives in their governing equations has garnered significant attention due to its remarkable ability to describe complex phenomena (Failla and Zingales, 2020). These include, for example, biological tissues, electrical properties of nerve cell membranes, arterial viscoelasticity (Craiem and Armentano, 2007; Magin, 2004, 2010; Guo et al., 2021; Torvik and Bagley, 1984); Lomnitz's law and seismic attenuation in geophysics (Wang and Guo, 2004; Pandey and Holm, 2016); the fractional Schrödinger equation (Laskin, 2002); fractional Fick's law for diffusion (Paradisi et al., 2001); and fractional viscoelastic models in multiscale, fractal, and porous media (Mashayekhi et al., 2018, 2019; Pahari and Oates, 2022; Oates et al., 2021; Gemant, 1938; Nutting, 1921; Torvik and Bagley, 1984; Szabo, 1994; Fellah et al., 2004; Stanisauskis et al., 2022), to name a few. Since the foundational work of Torvik and Bagley (1984), the modeling of complex media using fractional calculus has been widely pursued across disciplines, proving highly effective in explaining phenomena that defy classical theory and in predicting novel behaviors (Guo et al., 2021; Failla and Zingales, 2020; Monje et al., 2010; Rossikhin and Shitikova, 2009; Patnaik and Semperlotti, 2020; Ionescu et al., 2017; Drapaca and Sivaloganathan, 2012).

* Corresponding author.
E-mail addresses: kshiteej.jd@gmail.com (K.J. Deshmukh), liu.liping@rutgers.edu (L. Liu), psharma@central.uh.edu (P. Sharma).

https://doi.org/10.1016/j.jmps.2026.106740
Received 11 May 2026; Received in revised form 21 June 2026; Accepted 22 June 2026
Available online 30 June 2026
0022-5096/

A fractional differential equation is inherently nonlocal. For example, the *fractional Laplace equation* in d spatial dimensions with the spatial variable $\boldsymbol{x} \in \mathbb{R}^d$ can be written as:

$$(-\Delta)^{s/2} u(\boldsymbol{x}) = f(\boldsymbol{x}), \tag{1.1}$$

where $0 < s < 2$ and $(-\Delta)^{s/2}$ denotes the fractional Laplacian. This operator may be expressed in its integral form as:

$$(-\Delta)^{s/2} u(\boldsymbol{x}) = C_s \,\text{P.V.} \int_{\mathbb{R}^d} \frac{u(\boldsymbol{x}) - u(\boldsymbol{y})}{|\boldsymbol{x} - \boldsymbol{y}|^{d+s}} \, \mathrm{d}\boldsymbol{y}, \tag{1.2}$$

where P.V. denotes the Cauchy principal value and C_s is a normalization constant that appears in the definition of the fractional Laplacian (Di Nezza et al., 2012) (see Appendix B for more details on fractional Laplace operators). This should be contrasted with the conventional Laplace equation, which is purely local in nature. Such distinctions highlight why fractional calculus has emerged as a powerful framework for modeling nonlocality, memory effects, and long-range interactions in complex media (Adolfsson et al., 2005; Patnaik and Semperlotti, 2020; Failla and Zingales, 2020; Mashayekhi et al., 2018; Solheim et al., 2018; Stanisauskis et al., 2022).

Mechanics, notably, has a rich tradition of incorporating nonlocal behavior into its theoretical foundations. Early nonlocal elasticity theories, such as those developed by Kröner (1967), Eringen and Edelen (1972), sought to capture long-range cohesive forces and their effects on wave dispersion-features absent in classical elasticity. Another means of introducing (weak) nonlocality is via higher-order derivatives of field variables. Theories of higher-order strain gradient elasticity, originating from the seminal works of Toupin (1962), Mindlin (1964, 1965), Mindlin and Eshel (1968), Ericksen and Truesdell (1957), have gained popularity for their ability to model size-dependent phenomena across elasticity, plasticity, and related subfields.

However, a key limitation of these gradient theories is that they are grounded in integer-order calculus and consequently predict effective macroscopic properties that scale with integer powers of intrinsic length scales. In contrast, fractional-order models, which are inherently nonlocal, have found considerable success in describing materials where classical theories fall short (Ding et al., 2022; Patnaik et al., 2020; Patnaik and Semperlotti, 2020; Dahlberg and Ortiz, 2019; Ariza et al., 2024). A compelling example lies in the plasticity of thin films, where experimental data show that the yield strength scales with a *fractional* power of film thickness; behavior not explained by integer-order models. Fractional plasticity models (Dahlberg and Ortiz, 2019) account for this by relating the fractional order of the derivative directly to the observed scaling exponent.

Despite the widespread adoption of fractional calculus in modeling anomalous behavior, the physical origin of fractional operators in material models remains poorly understood. Often, integer-order derivatives are simply replaced with their fractional counterparts, and the exponent is treated as a fitting parameter. This might be adequate for reproducing empirical trends but lacks predictive power. This empirical approach leaves unanswered a key question: *Which specific microstructural features give rise to fractional behavior, and how do changes in microstructure affect the fractional model parameters?*

One theoretical pathway involves starting from an energy functional incorporating long-range interactions. This is typically modeled to decay with a power-law characterized by a fractional exponent. Variational methods then lead to Euler-Lagrange equations that naturally contain fractional derivatives, thereby rationalizing the emergence of fractional laws and size-dependent effects. In essence, nonlocal interactions at the microscale, especially those decaying with a power-law, can lead to macroscopic models governed by fractional differential equations. Separately, homogenization is known to yield effective nonlocal behavior in composite materials, and several studies have proposed nonlocal (or nonlocal adjacent) constitutive stress-strain relations via this route (Willis, 1981a, 1983, 1985; Luciano and Willis, 2003, 2005; Willis, 2011, 2019; Drugan and Willis, 1996; Milton, 2002; Deshmukh et al., 2022; Mukherjee et al., 2026; Forest and Sab, 1998). However, classical homogenization (Ponte Castaneda and Willis, 1988; Castañeda and Willis, 1995) is typically limited to periodic or random microstructures with rapidly (e.g., exponentially) decaying correlations, and it often assumes a slowly varying mean field.[1]

In this work, we directly address the underlying mechanism by which fractional derivatives emerge in material models. Specifically, we ask: *What forms of microstructural randomness produce a fractional-order response in the homogenized constitutive relations?* Our central contribution is to demonstrate that *fractional behavior can emerge purely from classical linear elasticity* at the microscale, without invoking any pre-assumed nonlocal interactions, provided the microstructure has a *power-law correlation*. This result provides an explanation of a sufficient mechanism for the origin of fractional constitutive behavior and establishes a direct link between the microstructural statistics and the order of the fractional derivative. In a recent work (Khandagale et al., 2024), using a statistical mechanics framework for modeling plasticity, the authors obtained the fractional exponent dictating the size-effects in thin film plasticity behavior by linking it to long-range microscopic interactions. In contrast, the present work makes no such assumptions

[1] We emphasize that the homogenization framework adopted in this work is the ensemble-averaged, finite-body framework of Willis (1981a), rather than the classical asymptotic homogenization framework. In classical asymptotic homogenization, under uniform ellipticity of the moduli and standard scale-separation assumptions, the leading effective response is local; in small-contrast expansions, the second-order correction is also local and depends on the microstructure through two-point statistics. Spatially nonlocal homogenized limits generally require more singular settings, such as high-contrast media or loss of uniform ellipticity, including media containing voids or effectively rigid phases (Camar-Eddine and Seppecher, 2003; Camar-Eddine and Milton, 2005; Milton, 2002). By contrast, in Willis' formulation, the effective constitutive law is defined through ensemble-averaged fields on a bounded body subject to specified boundary conditions. The resulting effective constitutive operator need not be local on this bounded domain. Consequently, the effective response in this framework can depend on the size and shape of the body, as well as on the imposed boundary conditions.

on microscopic interactions and thus provides a stronger fundamental principle for the origin of fractional calculus-based material models. A highlight of this work is the linking of material microstructure to the emergent fractional order (fractional exponent) of the governing equations. Thus, the proposed principle has implications beyond elasticity and can be extended to problems in conductivity, electromagnetism, viscoelasticity etc. for exploring emergent fractional models that could potentially lead to novel design strategies.

In the static setting, our effective constitutive law is derived using Willis' framework with a perturbative expansion in the elastic contrast (retaining terms up to second order). We show that when a two-phase random microstructure governed by classical linear elasticity is homogenized, it yields an effective fractional model if the phase correlation (or autocovariance) function exhibits a power-law decay. The order of the fractional derivative is directly linked to the exponent in this correlation. The resulting effective modulus exhibits fractional size dependence (dependent on the fractional exponent of the size)-a finding that is highly relevant to recent studies on thin-film plasticity and size-dependent mechanical behavior (Dahlberg and Ortiz, 2019; Ariza et al., 2024; Khandagale et al., 2024). The fractional size effect is specifically demonstrated for a simplified example of anti-plane elasticity. The emergent fractional constitutive law is also shown for the more general case of a linear 3D isotropic heterogeneous medium. In fact, we argue that, in general, we can obtain a fractional calculus-based description for any convolution-type nonlocal integral with a power-law kernel. This appears to be a fundamental new result that we have not found in the literature.

1.1. Map of the paper

The paper is structured to move from microstructure statistics to effective constitutive laws, and then to the two principal outcomes: (i) emergent fractional behavior, i.e., effective or macroscopic constitutive laws that contain fractional derivatives, and (ii) fractional size effects, i.e., effective property scaling with a fractional power of the feature size of the body. We begin in Section 2 by defining the two-phase random medium and introducing the statistical descriptors (indicator functions, probability functions, and the autocovariance) that encode the microstructural information used throughout the homogenization. Section 3 then sets up the elasticity problem and outlines the perturbation-based Willis framework that converts these statistical descriptors into ensemble-averaged (effective) field equations. Building on this, Section 4 derives the effective stress-strain relation in an explicit nonlocal operator form, making clear where microstructural correlations enter the macroscopic constitutive response.

In Section 5, we specialize the general nonlocal effective law to the *static* anti-plane setting, where the displacement is scalar, and the strain is $\boldsymbol{\epsilon} = \nabla u$. In this simplifying reduction, the effective constitutive response can be written as a *nonlocal operator* acting on the mean strain: a local (size-independent) part plus a correlation-induced correction that admits an explicit representation in terms of fractional operators. In particular, for a power-law autocovariance tail $\chi(r) \sim r^{-2\eta}$ with $\eta \in (0,1)$, the nonlocal correction takes an isotropic form built from a linear combination of fractional Laplacians and their derivatives, which schematically is

$$\boldsymbol{\mu}_* = \langle \mu \rangle \boldsymbol{I} + \boldsymbol{L}_{\text{loc}} + \text{const} \times \left(3\, \nabla\nabla(-\Delta)^{-(1-\eta)} + \boldsymbol{I}(-\Delta)^{\eta} \right),$$

thereby making transparent how the microstructural correlation exponent fixes the fractional orders appearing in the effective operator.

Using the above operator form, we then isolate the fractional (nonlocal) contribution and perform a scaling analysis on a bounded specimen (e.g., $\Omega = \Omega_R$). By prescribing a representative mean strain inside Ω_R that is geometrically self-similar[2] and extending it by zero outside, the fractional operators yield an explicit algebraic dependence on the domain size R. This leads to a fractional size-effect: the nonlocal contribution to the mean stress scales as

$$\langle \boldsymbol{\sigma} \rangle(\boldsymbol{x}) = \underbrace{\left(\langle \mu \rangle \boldsymbol{I} + \boldsymbol{L}_{\text{loc}} \right) \langle \boldsymbol{\epsilon} \rangle}_{\text{local contribution}} + \text{const} \times R^{-2\eta} \underbrace{\boldsymbol{\Theta}(\boldsymbol{x}/R)}_{\text{nonlocal contribution}},$$

so that the magnitude of the emergent nonlocal correction decays like $R^{-2\eta}$ while the spatial variation enters only through some function $\boldsymbol{\Theta}(\boldsymbol{x})$ of the dimensionless ratio $\boldsymbol{x}/R$. Section 6 analyzes the more general case of 3D linear isotropic elasticity to obtain the emergent fractional behavior that is much more complex than the simple example of anti-plane shear.

We close with a brief conclusion highlighting implications and extensions. Technical background on the statistical correlation functions and the fractional operator machinery used in the analysis is collected in the Appendices for reference.

2. The microstructure description

We begin by describing the heterogeneous or composite microstructure considered in this work, and detail some of the important terms characterizing the micro-structure that will be relevant to the analysis in the following section. We remark that the content of this section is not original and is summarized for completeness to make this work self-contained.

Consider a statistically homogeneous two-phase random medium occupying a finite (bounded) domain $\Omega \subset \mathbb{R}^d$ (with $d \geq 1$), with random distribution of pure phases $i = 1, 2$. When Fourier methods over $\mathbb{R}^d$ are used later, we interpret them either by extending ensemble-averaged fields by zero outside a bounded Ω (so the relevant fields are compactly supported) or, if $\Omega = \mathbb{R}^d$ is used as an idealization, in the standard tempered-distribution sense. Let ϕ_i, $\boldsymbol{L}_i$, and ρ_i denote the volume fraction, elastic modulus, and mass density of the i^{th} phase, respectively. Here, $\boldsymbol{L}_i$ denotes a fourth-order tensor with components $L^{(i)}_{klmn}$ $(k, l, m, n = 1, \dots, d)$. The i^{th}-phase occupies a volume $\Omega_i \in \Omega$, and $\Omega = \cup_{i=1}^{2}\ \Omega_i$. The 2-phase random medium is drawn from a sample space $\mathcal{P}(\alpha)$ with some probability

[2] That is, the shape stays the same as the domain is scaled

measure p, and the specific micro-geometry of any one sample depends on the parameter α. The micro-geometry of a particular realization α, can be modeled by the indicator (also called characteristic) functions $\mathcal{I}_i(\boldsymbol{x};\alpha)$ of the respective phases, where $i = 1, 2$, denotes the i^{th} phase, and $\mathcal{I}_i(\boldsymbol{x};\alpha) = 1$ if $\boldsymbol{x} \in \Omega_i$, otherwise 0.

2.1. Covariance function: statistical description of the micro-geometry

For a given $\boldsymbol{x}$, $\mathcal{I}_i(\boldsymbol{x};\alpha)$ is a random variable. In general, it is impossible to obtain $\mathcal{I}_i(\boldsymbol{x};\alpha)$ for all possible realizations α of the random medium. For any meaningful analysis we need to use certain "mean" quantities that can be realistically obtained. The derivations presented in this section follow closely to those in the book by Torquato et al. (2002). Here, the mean is the ensemble average taken over possible realizations α. One such mean quantity is the one-point correlation function denoted by $S_1^{(i)}(\boldsymbol{x})$ (also called the one-point probability function) which gives the probability that phase i is found at the point $\boldsymbol{x}$. For the phase i it is defined as the ensemble mean of the indicator function

$$S_1^{(i)}(\boldsymbol{x}) = \langle \mathcal{I}_i(\boldsymbol{x};\alpha) \rangle, \tag{2.1}$$

where $\langle \cdot \rangle$ denotes the ensemble average:

$$\langle (\cdot) \rangle = \int_{\mathcal{P}(\alpha)} (\cdot) p(\,\mathrm{d}\alpha).$$

A 2-point probability (correlation) function $S_2^{(i)}(\boldsymbol{x}_1, \boldsymbol{x}_2)$ for the i^{th} phase gives the probability of finding phase i at points $\boldsymbol{x}_1$ and $\boldsymbol{x}_2$, and can be obtained from the relation

$$S_2^{(i)}(\boldsymbol{x}_1, \boldsymbol{x}_2) = \langle \mathcal{I}_i(\boldsymbol{x}_1;\alpha)\, \mathcal{I}_i(\boldsymbol{x}_2;\alpha) \rangle. \tag{2.2}$$

More generally, the two-point probability function with potentially dissimilar phases at the two ends is defined as

$$S_2^{(ij)}(\mathbf{x}_1, \mathbf{x}_2) = \langle \mathcal{I}_i(\mathbf{x}_1;\alpha)\, \mathcal{I}_j(\mathbf{x}_2;\alpha) \rangle, \tag{2.3}$$

which represents the probability of simultaneously finding phase i at position $\mathbf{x}_1$ and phase j at position $\mathbf{x}_2$. By (2.3) we see that

$$S_2^{(ii)} = S_2^{(i)}, \qquad S_2^{(12)}(\boldsymbol{x}_1, \boldsymbol{x}_2) = S_1^{(1)}(\boldsymbol{x}_1) - S_2^{(1)}(\boldsymbol{x}_1, \boldsymbol{x}_2). \tag{2.4}$$

In this work, we assume that the microstructure is statistically homogeneous and isotropic. A random medium is said to be statistically homogeneous if the probability functions do not depend on the absolute positions $(\boldsymbol{x}_1, \boldsymbol{x}_2)$, and instead depend on their relative position vector as $\boldsymbol{x}_1 - \boldsymbol{x}_2$. Statistical isotropy implies direction independence or rotational invariance, and hence the probability functions depend on relative distances $|\boldsymbol{x}_1 - \boldsymbol{x}_2|$, i.e., they are translation invariant for an infinite medium. This implies that the one-point probability function in (2.1) is independent of $\boldsymbol{x}$ and takes a constant value equal to the volume fraction:

$$S_1^{(i)} = \phi_i \qquad (i = 1, 2). \tag{2.5}$$

The two-point probability function in (2.4) depends only on the relative distances between the points, $|\boldsymbol{x}_1 - \boldsymbol{x}_2|$. Hence, $S_2^{(i)}(\boldsymbol{x}_1, \boldsymbol{x}_2) = S_2^{(i)}(|\boldsymbol{x}_1 - \boldsymbol{x}_2|)$.

Let the relative position vector of two points be denoted by $\boldsymbol{r} = \boldsymbol{x}_1 - \boldsymbol{x}_2$, and $r = |\boldsymbol{r}|$. It is convenient to introduce the *autocovariance function* $\chi(r)$, defined as

$$\chi(r) = \langle \left[\left(\mathcal{I}_1(\mathbf{x_1}) - \phi_1 \right) \left(\mathcal{I}_1(\mathbf{x_1} + \mathbf{r}) - \phi_1 \right) \right] \rangle = S_2^{(1)}(r) - \phi_1^2,$$

It can be shown that the autocovariance of phase-1 is equal to the autocovariance of phase-2 (see (A.9) in Appendix A). Any realizable $\chi(|\boldsymbol{x}_1 - \boldsymbol{x}_2|)$ is subject to some (necessary but not sufficient) non-negative conditions (Torquato et al., 2002). We observe that in the limit $|\boldsymbol{x}_1 - \boldsymbol{x}_2| \to 0$,

$$\lim_{|\boldsymbol{x}_1 - \boldsymbol{x}_2| \to 0} \chi(|\boldsymbol{x}_1 - \boldsymbol{x}_2|) = \lim_{|\boldsymbol{x}_1 - \boldsymbol{x}_2| \to 0} S_2^{(1)}(|\boldsymbol{x}_1 - \boldsymbol{x}_2|) - \phi_1^2 = \phi_1 - \phi_1^2 = \phi_1 \phi_2. \tag{2.6}$$

If there is no long-range order — meaning that as $|\mathbf{x}_1 - \mathbf{x}_2| \to \infty$, the events at $\mathbf{x}_1$ and $\mathbf{x}_2$ become statistically independent — then we have

$$\lim_{|\boldsymbol{x}_1 - \boldsymbol{x}_2| \to \infty} S_2^{(1)}(|\boldsymbol{x}_1 - \boldsymbol{x}_2|) = \langle \mathcal{I}_1(\boldsymbol{x}_1) \rangle \langle \mathcal{I}_1(\boldsymbol{x}_2) \rangle = \phi_1^2 \qquad \Rightarrow \qquad \lim_{r \to +\infty} \chi(r) = 0. \tag{2.7}$$

Due to the binary nature of $\mathcal{I}_i(\boldsymbol{x})$, the bounds on $S_2^{(i)}$ are easily found to be, $0 < S_2^{(i)} < \phi_i$. Using these bounds in (A.9), we can find bounds on χ which can be written as,

$$-\min\{\phi_1^2, \phi_2^2\} < \chi(r) < \phi_1 \phi_2 \tag{2.8}$$

Another condition is on the slope of $\chi(r)$ being negative for all non-trivial volume fractions (Yeong and Torquato, 1998; Torquato et al., 2002), i.e.,

$$\left.\frac{\mathrm{d}\chi(r)}{\mathrm{d}r}\right|_{r=0} < 0. \tag{2.9}$$

For more details on the properties of $\chi(\boldsymbol{r})$, and n–point probability functions of random heterogeneous media, we refer the readers to the book by Torquato et al. (2002).

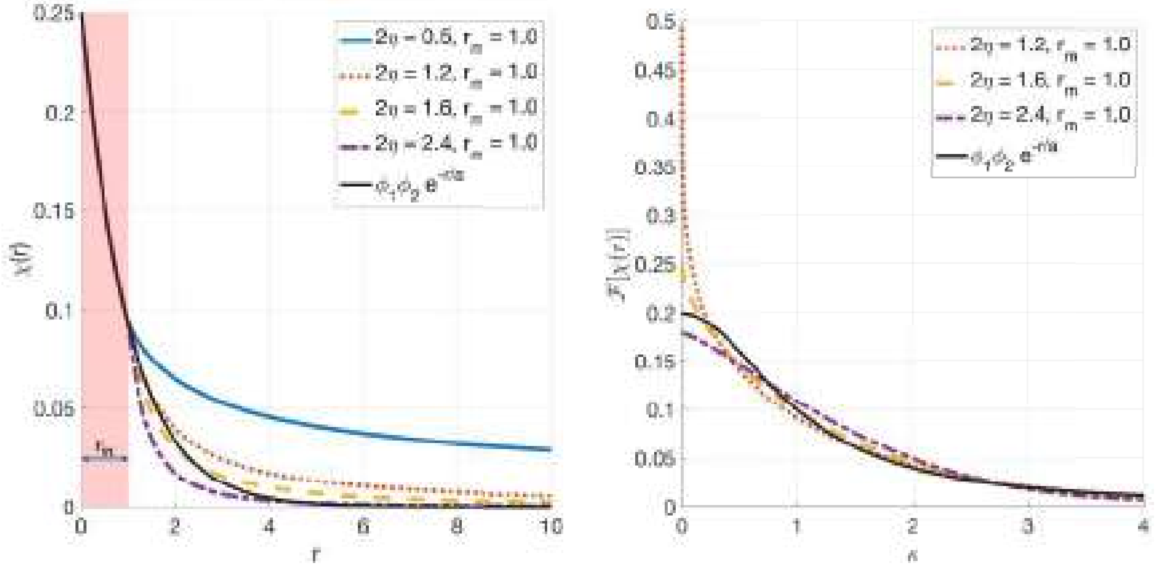

(a) (b)

Fig. 1. Autocovariance functions with exponential behavior in the core region (shaded in red) and a power-law decay outside the core region are shown: (a) $\chi(r)$ in real-space, (b) Fourier transformed autocovariance $\mathcal{F}[\chi]$ vs. the wavevector κ. Keeping all other parameters fixed, $a = 1, r_m = 1, \phi_1\phi_2 = 0.25$, only the power-law exponent is varied. The value of the power-law exponent 2η determines the rate of decay, making it slower or faster. The purely exponential decay is shown by the solid black curve, which is typical of the commonly studied two-phase random composites. The Fourier transform of χ for $2\eta = 0.5$ is not defined and is not shown in the Fourier space.

Generally, the function $\chi(r)$ is assumed to decay very rapidly as r increases, and is typically of the exponential form $e^{-r/a}$, where a is the decay length scale. Here, we consider the case where the autocovariance has a slower power-law decay (algebraic). Unlike the exponential correlation, power-law correlations do not have a finite correlation length scale. Power-law distributions are abundantly seen in many naturally occurring phenomena like galaxy distributions, biological structures (Labini et al., 2007; Qin and Colwell, 2018; Mori et al., 2020), and porous materials (Chen and Torquato, 2018). By taking into account the conditions on χ stated above, we propose the following form of $\chi(r)$:

$$\chi(r) = \begin{cases} \phi_1\phi_2\ e^{-r/a} = A_e e^{-r/a}, & \text{if } \ 0 \le r \le r_m \\ \\ \phi_1\phi_2 r_m^{2\eta}\ \frac{e^{-r_m/a}}{r^{2\eta}} = A_p(r_m) r_m^{2\eta} \frac{1}{r^{2\eta}}, & \text{if } \ r > r_m \end{cases} \tag{2.10}$$

where, $A_e = \phi_1\phi_2$, $A_p = \phi_1\phi_2 e^{-r_m/a}$, and $r_m, a > 0$ are constants. For more details on the derivation of the statistical quantities, see Appendix A. The above form of the piecewise autocovariance allows for a core part inside a sphere of certain radius r_m, which is taken to be of the exponential form. The exterior region of the core, outside the sphere with radius r_m, has a power-law decay, and the proposed form of χ ensures continuity of the autocovariance at the spherical surface of radius r_m.

Fig. 1(a)-(b) shows the autocovariance functions in real-space and Fourier-space plotted for different values of the power-law exponent 2η. The core radius is fixed at $r_m = 1$ and the volume fractions are arbitrarily chosen such that $\phi_1\phi_2 = 0.25$. For reference, we also show the pure exponential autocovariance (solid black curve), which is typically observed in the study of most random composites. The power-law exponent 2η determines the rate of decay of χ. Note that for χ with $\eta = 0.5 < 1$ (shown in blue), the Fourier transform of the autocovariance function denoted by $\mathcal{F}[\chi](\kappa)$ is not well-defined as the integral diverges. Hence, although we show the real-space form of χ in Fig. 1(a), we have not shown its corresponding Fourier plot in Fig. 1(b). We can notice from Fig. 1(a)-(b) that, as is well-known, the wider the spread of χ in real-space, the more localized (narrow spread) it is in the Fourier space.

2.2. Statistical description of the microstructure moduli

The elastic modulus of the inhomogeneous medium in the realization α, represented by $\boldsymbol{L}(\boldsymbol{x};\alpha)$, varies with position $\boldsymbol{x}$, and can be expressed using the indicator functions as,

$$\boldsymbol{L}(\boldsymbol{x};\alpha) = \sum_{i=1}^{2} \boldsymbol{L}_i \mathcal{I}_i(\boldsymbol{x};\alpha), \quad \Longrightarrow \quad \langle \boldsymbol{L}\rangle(\boldsymbol{x}) = \sum_{i=1}^{2} \boldsymbol{L}_i S_1^{(i)}(\boldsymbol{x}). \tag{2.11}$$

The linear elastic constitutive relation between stress and strain is given by

$$\boldsymbol{\sigma}(\boldsymbol{x};\alpha) = \boldsymbol{L}(\boldsymbol{x};\alpha)\boldsymbol{\epsilon}(\boldsymbol{x};\alpha), \qquad \boldsymbol{\epsilon} = \frac{1}{2}(\nabla \boldsymbol{u} + (\nabla \boldsymbol{u})^{\top}) \tag{2.12}$$

where $\boldsymbol{\sigma}, \boldsymbol{\epsilon}$, and $\boldsymbol{u}$ is respectively the elastic stress, strain, and displacement. Suppose that the overall heterogeneous body Ω is subject to an applied body force $\boldsymbol{f}$ and the boundary displacement is prescribed as $\boldsymbol{u} = \boldsymbol{u}_0$ on $\partial\Omega$. Then the equilibrium equation for the inhomogeneous elastic body can be written as

$$\begin{aligned} &\operatorname{div} \boldsymbol{\sigma}(\boldsymbol{x};\alpha) + \boldsymbol{f}(\boldsymbol{x}) = \boldsymbol{0} \quad \text{in} \quad \Omega, \\ &\boldsymbol{u}(\boldsymbol{x}) = \boldsymbol{u}_0 \quad \text{on} \quad \partial\Omega. \end{aligned} \tag{2.13}$$

which is also the Euler-Lagrange equation of the variational principle:

$$\min_{\boldsymbol{u}} \left\{ I[\boldsymbol{u}] = \int_{\Omega} (\frac{1}{2}\nabla \boldsymbol{u} \cdot \boldsymbol{L}\nabla \boldsymbol{u} - \boldsymbol{f} \cdot \boldsymbol{u}) : \ \boldsymbol{u} = \boldsymbol{u}_0 \text{ on } \partial\Omega \right\}. \tag{2.14}$$

Here and subsequently, we omit the explicit dependence on $\mathbf{x}$ and α for brevity, reintroducing it when necessary for clarity.

3. Homogenization using perturbation theory *à la* Willis

Our goal is to find an effective description of the equilibrium equations in terms of an effective modulus denoted by $\boldsymbol{L}_*$. Willis, in several of his works (Willis, 1981a,b, 1983, 1985; Drugan and Willis, 1996; Willis, 2011, 2019), has proposed homogenization techniques and variational principles to determine the static and dynamic effective properties of heterogeneous media. In this section, following the methodology of Willis (1983), we briefly summarize the macroscopic governing equations and the effective modulus operator for elasticity within a perturbation-based framework. These equations serve as the starting point of our work. The elastic modulus, stress, strain, and displacement fields are all dependent on the realization α of the sample under consideration. To get an effective prescription, we will look for relations connecting the ensemble averages over all realizations α of the sample. Taking the ensemble average of (2.13) over all realizations yields,

$$\langle \boldsymbol{\sigma} \rangle(\boldsymbol{x}) = \langle \boldsymbol{L}(\boldsymbol{x})\boldsymbol{\epsilon}(\boldsymbol{x}) \rangle =: \boldsymbol{L}_*(\langle \boldsymbol{\epsilon} \rangle(\boldsymbol{x})). \tag{3.1}$$

The above equation also defines the *effective modulus* or effective operator $\boldsymbol{L}_*$, which relates the mean strain field to the mean stress field. In the Willis framework used here, $\boldsymbol{L}_*$ should be understood as an effective *operator* defined through ensemble-averaged fields on a finite domain Ω subject to prescribed boundary conditions. Consequently, for finite Ω the kernel representation of $\boldsymbol{L}_*$ is, in general, dependent on the chosen volume element and on the imposed boundary conditions, and the associated nonlocality is a finite-volume/general-BC effect. A classical local homogenized modulus (obtained from asymptotic homogenization) may be recovered in regimes where an appropriate infinite-domain / long-wavelength limit exists and the resulting effective response becomes independent of boundary conditions and of the particular choice of Ω.

We will characterize the *effective operator* $\boldsymbol{L}_*$ by a perturbative method. To proceed, we introduce a reference homogeneous medium $\boldsymbol{L}_0$ and denote by $\boldsymbol{\sigma}_0$, $\boldsymbol{\epsilon}_0$, and $\boldsymbol{u}_0$ the corresponding solution for the homogeneous medium subject to the same boundary condition as in $(2.13)_2$. For simplicity, we choose the reference medium's modulus as $\boldsymbol{L}_0 = \langle \boldsymbol{L} \rangle$. Denote by $\boldsymbol{G}(\boldsymbol{x}, \boldsymbol{x}')$ the Green's function for the homogeneous reference body satisfying

$$\begin{cases} \frac{\partial}{\partial x_m}\left[(L_0)_{imlk} G_{lj,k}(\boldsymbol{x}, \boldsymbol{x}')\right] = -\delta(\boldsymbol{x} - \boldsymbol{x}')\delta_{ij} & \text{in } \Omega, \\ G_{ij}(\boldsymbol{x}, \boldsymbol{x}') = 0 & \forall\ \boldsymbol{x} \in \partial\Omega, \end{cases} \tag{3.2}$$

where $\delta_{ij} = 1$ if $i = j$ and vanishes if $i \neq j$, and $\delta(\boldsymbol{x})$ is the Dirac function. In terms of the Green's function (3.2), we have

$$u_{0i}(\boldsymbol{x}) = \int_{\Omega} G_{ij}(\boldsymbol{x}, \boldsymbol{x}') f_j(\boldsymbol{x}')\, \mathrm{d}\boldsymbol{x}'.$$

For the inhomogeneous problem (2.12)–(2.13), let

$$\boldsymbol{\tau}(\boldsymbol{x}) = (\boldsymbol{L} - \boldsymbol{L}_0)\boldsymbol{\epsilon}(\boldsymbol{x}) = \delta \boldsymbol{L}\boldsymbol{\epsilon}(\boldsymbol{x}) \qquad\qquad (\delta \boldsymbol{L} = \boldsymbol{L} - \boldsymbol{L}_0) \tag{3.3}$$

be the stress polarization. Upon rewriting $(2.13)_1$ as

$$\operatorname{div}((\boldsymbol{L} - \boldsymbol{L}_0 + \boldsymbol{L}_0)\boldsymbol{\epsilon}) = \operatorname{div} \boldsymbol{L}_0\boldsymbol{\epsilon} + \operatorname{div} \boldsymbol{\tau} = -\boldsymbol{f}, \tag{3.4}$$

we see that the solution to (3.4) can be written in terms of the Green's function (3.2) for the homogeneous reference medium as

$$u_i(\boldsymbol{x}) = \int_{\Omega} G_{ij}(\boldsymbol{x}, \boldsymbol{x}')(\operatorname{div}_{\boldsymbol{x}'} \boldsymbol{\tau})_j(\boldsymbol{x}')\, \mathrm{d}\boldsymbol{x}' + u_{0i}(\boldsymbol{x}). \tag{3.5}$$

Recall the kinematic relation between strain and displacement (Cf. (2.12)). Differentiating (3.5) w.r.t $\boldsymbol{x}$ and symmetrizing, we get the strain $\boldsymbol{\epsilon}$ in the original material in terms of strain in the reference medium $\boldsymbol{\epsilon}_0$ and the stress polarization

$$\boldsymbol{\epsilon} = \boldsymbol{\epsilon}_0 - \boldsymbol{\Gamma}\boldsymbol{\tau}, \tag{3.6}$$

where

$$(\boldsymbol{\Gamma}\boldsymbol{\tau})_{ij} = \int_{\Omega} \frac{1}{2}\Big(\frac{\partial^2 G_{ik}(\boldsymbol{x},\boldsymbol{x}')}{\partial x_j \partial x'_l} + \frac{\partial^2 G_{jk}(\boldsymbol{x},\boldsymbol{x}')}{\partial x_i \partial x'_l} \Big)(\boldsymbol{\tau})_{kl}(\boldsymbol{x}')d\boldsymbol{x}' \tag{3.7}$$

is a nonlocal linear operator, i.e., a spatial convolution. Combining relations (3.6) and (3.3), we get

$$\boldsymbol{\epsilon} = \boldsymbol{\epsilon}_0 - \boldsymbol{\Gamma}(\delta \boldsymbol{L}\boldsymbol{\epsilon}) \tag{3.8}$$

In Eq. (3.8), if $\boldsymbol{L}(\boldsymbol{x}) - \boldsymbol{L}_0 \equiv \delta\boldsymbol{L}(\boldsymbol{x})$ is small, we can apply perturbation theory to perform further analysis. To simplify the analysis we choose the reference medium with $\boldsymbol{L}_0 = \langle \boldsymbol{L}\rangle$. Now, we express the actual strain in (3.8) as a perturbation about the mean,

$$\boldsymbol{\epsilon} = \langle\boldsymbol{\epsilon}\rangle + \delta\boldsymbol{\epsilon}, \tag{3.9}$$

Ensemble averaging relation (3.8) gives,

$$\langle\boldsymbol{\epsilon}\rangle = \boldsymbol{\epsilon}_0 - \boldsymbol{\Gamma}\langle\delta\boldsymbol{L}\delta\boldsymbol{\epsilon}\rangle. \tag{3.10}$$

Subtracting (3.10) from (3.8) and using (3.9) we get,

$$\delta\boldsymbol{\epsilon} = -\boldsymbol{\Gamma}\delta\boldsymbol{L}\langle\boldsymbol{\epsilon}\rangle - \boldsymbol{\Gamma}(\delta\boldsymbol{L}\delta\boldsymbol{\epsilon} - \langle\delta\boldsymbol{L}\delta\boldsymbol{\epsilon}\rangle) \tag{3.11}$$

We assumed $\delta\boldsymbol{L}$ to be small, then $\delta\boldsymbol{\epsilon}$ is also small, and the relation in (3.11) can be applied iteratively to get,

$$\begin{aligned} &\delta\boldsymbol{\epsilon} = -\boldsymbol{\Gamma}\delta\boldsymbol{L}\langle\boldsymbol{\epsilon}\rangle - \boldsymbol{\Gamma}\Big(\delta\boldsymbol{L}(-\boldsymbol{\Gamma}\delta\boldsymbol{L}\langle\boldsymbol{\epsilon}\rangle - \boldsymbol{\Gamma}(\delta\boldsymbol{L}\delta\boldsymbol{\epsilon} - \langle\delta\boldsymbol{L}\delta\boldsymbol{\epsilon}\rangle)) - \langle\delta\boldsymbol{L}(-\boldsymbol{\Gamma}\delta\boldsymbol{L}\langle\boldsymbol{\epsilon}\rangle - \boldsymbol{\Gamma}(\delta\boldsymbol{L}\delta\boldsymbol{\epsilon} - \langle\delta\boldsymbol{L}\delta\boldsymbol{\epsilon}\rangle))\rangle\Big) \\ \implies &\delta\boldsymbol{\epsilon} = -\boldsymbol{\Gamma}\delta\boldsymbol{L}\langle\boldsymbol{\epsilon}\rangle + \boldsymbol{\Gamma}\Big(\delta\boldsymbol{L}\boldsymbol{\Gamma}\delta\boldsymbol{L} - \langle\delta\boldsymbol{L}\boldsymbol{\Gamma}\delta\boldsymbol{L}\rangle\Big)\langle\boldsymbol{\epsilon}\rangle + \dots \end{aligned} \tag{3.12}$$

We can now rewrite the expression (3.1) for mean stress in terms of the mean and perturbed strains as,

$$\langle\boldsymbol{\sigma}\rangle = \langle\boldsymbol{L}\boldsymbol{\epsilon}\rangle = \boldsymbol{L}_*\langle\boldsymbol{\epsilon}\rangle = \langle\boldsymbol{L}\rangle\langle\boldsymbol{\epsilon}\rangle + \langle\delta\boldsymbol{L}\delta\boldsymbol{\epsilon}\rangle. \tag{3.13}$$

Substituting (3.12) in (3.13), the mean stress upto second-order can be written as,

$$\begin{aligned} &\langle\boldsymbol{\sigma}\rangle = \boldsymbol{L}_*\langle\boldsymbol{\epsilon}\rangle = \langle\boldsymbol{L}\rangle\langle\boldsymbol{\epsilon}\rangle - \Big(\langle\delta\boldsymbol{L}\boldsymbol{\Gamma}\delta\boldsymbol{L}\rangle - \langle\delta\boldsymbol{L}\boldsymbol{\Gamma}\delta\boldsymbol{L}\boldsymbol{\Gamma}\delta\boldsymbol{L}\rangle + \dots\Big)\langle\boldsymbol{\epsilon}\rangle \\ \implies &\langle\boldsymbol{\sigma}\rangle(\boldsymbol{x}) \approx \langle\boldsymbol{L}\rangle(\boldsymbol{x})\langle\boldsymbol{\epsilon}\rangle(\boldsymbol{x}) - \big(\langle\delta\boldsymbol{L}(\boldsymbol{x})\boldsymbol{\Gamma}(\boldsymbol{x},\boldsymbol{x}')\delta\boldsymbol{L}(\boldsymbol{x}')\rangle\big)\langle\boldsymbol{\epsilon}\rangle(\boldsymbol{x}). \end{aligned} \tag{3.14}$$

Thus, the expression approximating the effective operator $\boldsymbol{L}_*$ is obtained as,

$$\boldsymbol{L}_*(\boldsymbol{x}) \approx \langle\boldsymbol{L}\rangle(\boldsymbol{x}) - \langle\delta\boldsymbol{L}(\boldsymbol{x})\boldsymbol{\Gamma}(\boldsymbol{x},\boldsymbol{x}')\delta\boldsymbol{L}(\boldsymbol{x}')\rangle. \tag{3.15}$$

In the expression above we have omitted the higher order terms in the perturbation expansion. The effective modulus is a nonlocal operator which has a local contribution from the mean of the moduli of the constituent phases, and a nonlocal contribution from the second term. The second term operates as a spatial convolution as stated in (4.1) below. The effective governing equations at this point can be written in terms of the effective modulus by taking the ensemble mean of (2.13) as,

$$\begin{aligned} &\operatorname{div}\langle\boldsymbol{\sigma}\rangle + \boldsymbol{f} = \boldsymbol{0} \quad \text{in} \quad \boldsymbol{\Omega}, \\ \implies &\operatorname{div}\boldsymbol{L}_*\langle\boldsymbol{\epsilon}\rangle + \boldsymbol{f} = \boldsymbol{0} \quad \text{in} \quad \boldsymbol{\Omega}, \end{aligned} \tag{3.16}$$

Note that until this point we have not used information on the form of the autocovariance χ, and the problem is still general in that sense. Alternative ways of determining the effective modulus through variational principles were given by Willis (1981a, 1983, 1985), Drugan and Willis (1996), Willis (2011, 2019) by connecting the Hashin-Shtrikman variational principles to classical energy principles.

4. The nonlocal effective operator for 3D isotropic elasticity

As discussed in the previous section the effective modulus $\boldsymbol{L}_*$, has a nonlocal contribution from the second term. We now focus on the second term to further analyze and derive a more specific form for it. Using the expression (2.11) for the modulus in the second term of (3.15) we obtain

$$\langle\delta\boldsymbol{L}\boldsymbol{\Gamma}\delta\boldsymbol{L}\rangle\langle\boldsymbol{\epsilon}\rangle(\boldsymbol{x}) = \sum_{(i,j)=1}^{2} \boldsymbol{L}_i \int_{\Omega} \boldsymbol{\Gamma}(\boldsymbol{x},\boldsymbol{x}')\boldsymbol{L}_j\Big(S_2^{(ij)}(\boldsymbol{x},\boldsymbol{x}') - S_1^{(i)}(\boldsymbol{x})S_1^{(j)}(\boldsymbol{x}')\Big)\langle\boldsymbol{\epsilon}\rangle(\boldsymbol{x}')\,\mathrm{d}\boldsymbol{x}'. \tag{4.1}$$

If the mean strain varies on a length scale much larger than the effective support/correlation length of the kernel in (4.1), then we may approximate $\langle\boldsymbol{\epsilon}\rangle(\boldsymbol{x}') \approx \langle\boldsymbol{\epsilon}\rangle(\boldsymbol{x})$, yielding a local constitutive approximation. This is a long-wavelength approximation and is not generally valid for kernels with long-range correlations. At this point, however, we *do not* restrict ourselves to slowly varying mean fields.

Next, we focus on the probability functions in (4.1), and our assumption of statistical homogeneity, allows the two-point correlation functions to be written as $S_2^{(ij)}(\boldsymbol{x},\boldsymbol{x}') = S_2^{(ij)}(\boldsymbol{x}-\boldsymbol{x}')$, and the one-point correlation functions take constant values equal to the volume fractions of the corresponding phases, i.e., $S_1^{(i)}(\boldsymbol{x}) = \phi_i$. Then, the probability terms in (4.1) can be written in terms of the autocovariance function denoted by $\chi(|\boldsymbol{x}-\boldsymbol{x}'|)$ using the relation (2.4) (for derivations see (A.9) and (A.4) from Appendix A). Specifically, we get,

$$\begin{aligned} S_2^{(11)}(\boldsymbol{x},\boldsymbol{x}') - S_1^{(1)}(\boldsymbol{x})S_1^{(1)}(\boldsymbol{x}') &= S_2^{(22)}(\boldsymbol{x},\boldsymbol{x}') - S_1^{(2)}(\boldsymbol{x})S_1^{(2)}(\boldsymbol{x}') = \chi(|\boldsymbol{x}-\boldsymbol{x}'|), \\ S_2^{(12)}(\boldsymbol{x},\boldsymbol{x}') - S_1^{(1)}(\boldsymbol{x})S_1^{(2)}(\boldsymbol{x}') &= S_2^{(21)}(\boldsymbol{x},\boldsymbol{x}') - S_1^{(2)}(\boldsymbol{x})S_1^{(1)}(\boldsymbol{x}') = -\chi(|\boldsymbol{x}-\boldsymbol{x}'|). \end{aligned} \tag{4.2}$$

Using these relations in (4.1) and expanding the summation gives,

$$\begin{aligned} \langle \delta \boldsymbol{L} \boldsymbol{\Gamma} \delta \boldsymbol{L} \rangle \langle \boldsymbol{\epsilon} \rangle &= \sum_{i,j} \boldsymbol{L}_i \int_\Omega \boldsymbol{\Gamma}(\boldsymbol{x},\boldsymbol{x}') \boldsymbol{L}_j \left(S_2^{(ij)}(\boldsymbol{x},\boldsymbol{x}') - S_1^{(i)}(\boldsymbol{x}) S_1^{(j)}(\boldsymbol{x}') \right) \langle \boldsymbol{\epsilon} \rangle(\boldsymbol{x}') \, \mathrm{d}\boldsymbol{x}' \\ &= \int_\Omega \triangle \mathbf{L} \boldsymbol{\Gamma}(\boldsymbol{x},\boldsymbol{x}') \triangle \mathbf{L} \chi(|\boldsymbol{x}-\boldsymbol{x}'|) \langle \boldsymbol{\epsilon} \rangle(\boldsymbol{x}') \, \mathrm{d}\boldsymbol{x}', \end{aligned} \tag{4.3}$$

where $\triangle \mathbf{L} = \boldsymbol{L}_1 - \boldsymbol{L}_2$ is the stiffness tensor difference between the two phases.

To further simplify the expression, we make the following observations and assumptions:

1. **Local singular structure of the reference Green operator.** Let $\boldsymbol{G}_\Omega(\boldsymbol{x},\boldsymbol{x}')$ denote the Green's function of the homogeneous reference medium posed on the bounded domain $\Omega \subset \mathbb{R}^d$ with the prescribed boundary conditions, and let $\boldsymbol{G}(\boldsymbol{x}-\boldsymbol{x}')$ denote the corresponding free-space (infinite-medium) Green's function on $\mathbb{R}^d$. The operator $\boldsymbol{\Gamma}_\Omega$ constructed from $\boldsymbol{G}_\Omega$ (via the second-derivative) has a bulk singularity of order $|\boldsymbol{x}-\boldsymbol{x}'|^{-d}$ as $\boldsymbol{x} \to \boldsymbol{x}'$. Accordingly, the singularity of $\boldsymbol{\Gamma}_\Omega$ is more explicitly stated by writing the nonlocal operator in the form,

$$\boldsymbol{\Gamma}_\Omega(\boldsymbol{x},\boldsymbol{x}') = \frac{\mathcal{G}(\boldsymbol{x},\boldsymbol{x}')}{|\boldsymbol{x}-\boldsymbol{x}'|^d} + \boldsymbol{K}(\boldsymbol{x},\boldsymbol{x}'), \tag{4.4}$$

where $\mathcal{G}$ is a bounded fourth-order tensor-valued function on the unit sphere (no poles). The *remainder* kernel, $\boldsymbol{K}_R$ is non-singular (smooth, no pole at $\boldsymbol{x}=\boldsymbol{x}'$) in the bulk and encodes the boundary-correction effects. For instance, in linear isotropic elasticity in $\mathbb{R}^d$, the free-space Green's function $\boldsymbol{G}$ has the form

$$\boldsymbol{G}(\boldsymbol{x}-\boldsymbol{x}') = A\, \boldsymbol{I}\, \nabla^2 |\boldsymbol{x}-\boldsymbol{x}'| + B\, \nabla\nabla |\boldsymbol{x}-\boldsymbol{x}'|, \tag{4.5}$$

where, A, B are some real constants related to the material's lame parameters, and we can see that differentiating twice yields the singular behavior $|\boldsymbol{x}-\boldsymbol{x}'|^{-d}$.
2. **Bulk-kernel approximation for the nonlocal operator.** For most finite geometries Ω, obtaining $\boldsymbol{G}_\Omega$ (and hence $\boldsymbol{\Gamma}_\Omega$) may be difficult. We therefore simplify by adopting a *bulk-body approximation* in which the nonlocal constitutive kernel is approximated by its translation-invariant infinite-medium counterpart:

$$\boldsymbol{\Gamma}_\Omega(\boldsymbol{x},\boldsymbol{x}') \approx \boldsymbol{\Gamma}(\boldsymbol{x}-\boldsymbol{x}'), \qquad \boldsymbol{\Gamma}(\boldsymbol{x}-\boldsymbol{x}') := \frac{\mathcal{G}(\boldsymbol{x},\boldsymbol{x}')}{|\boldsymbol{x}-\boldsymbol{x}'|^d}. \tag{4.6}$$

This approximation is justified for interior (bulk) response because the boundary correction $\boldsymbol{K}_R$ in (4.4) is non-singular and does not modify the local singular structure that determines the fractional order obtained from the power-law tail of χ. Consequently, using $\boldsymbol{\Gamma}$ affects only smooth and other geometry-dependent lower-order corrections, while preserving the emergent fractional scaling.
3. **Finite-domain implementation and size dependence.** Although (4.6) uses the infinite-medium kernel, the specimen remains finite through the domain of integration and the exterior/boundary data imposed on the macroscopic field (e.g., via a compactly supported or prescribed extension outside Ω). Therefore, finite-size effects enter through truncation by Ω and the associated exterior/boundary condition, and are not in contradiction with the bulk-kernel approximation. In particular, when $\chi(r)$ has a power-law tail, the resulting nonlocal contribution scales algebraically with the specimen size, yielding the fractional size-effect reported in Eq. (5.37).

With the above approximations, we now use the form of autocovariance given in (2.10), with the value of η restricted to the limits such that $\eta \in (0,1)$, and substitute in (4.3).

Then, splitting the integral in (4.3) into a core region where $r \le r_m$, and the exterior where $r > r_m$ we get,

$$\begin{aligned} &\triangle \mathbf{L} \int_\Omega \boldsymbol{\Gamma}(\boldsymbol{x},\boldsymbol{x}') \triangle \mathbf{L} \chi(|\boldsymbol{x}-\boldsymbol{x}'|) \langle \boldsymbol{\epsilon} \rangle(\boldsymbol{x}') \, \mathrm{d}\boldsymbol{x}' \\ &= A_e \triangle \mathbf{L} \int_{r \le r_m} \frac{\mathcal{G}(\boldsymbol{x},\boldsymbol{x}')}{|\boldsymbol{x}-\boldsymbol{x}'|^d} \triangle \mathbf{L} e^{(-|\boldsymbol{x}-\boldsymbol{x}'|/a)} \langle \boldsymbol{\epsilon} \rangle(\boldsymbol{x}') \, \mathrm{d}\boldsymbol{x}' + A_p r_m^{2\eta} \triangle \mathbf{L} \int_{r > r_m} \frac{\mathcal{G}(\boldsymbol{x},\boldsymbol{x}')}{|\boldsymbol{x}-\boldsymbol{x}'|^{d+2\eta}} \triangle \mathbf{L} \langle \boldsymbol{\epsilon} \rangle(\boldsymbol{x}') \, \mathrm{d}\boldsymbol{x}' \end{aligned} \tag{4.7}$$

In the core region, $r < r_m$, for small r_m we can approximate $\langle \boldsymbol{\epsilon} \rangle(\boldsymbol{x}') \approx \langle \boldsymbol{\epsilon} \rangle(\boldsymbol{x})$, so the integral with respect to $\boldsymbol{x}'$ in the first term is reduced to a local tensor operating on $\langle \boldsymbol{\epsilon} \rangle(\boldsymbol{x})$. The second integral gives the nonlocal contribution of $\langle \boldsymbol{\epsilon} \rangle(\boldsymbol{x}')$ to the mean stress, with the kernel decaying as a power-law. The second integral on the right hand side in (4.7), is evaluated on the exterior of the core, i.e., for $r > r_m$. We approximate this integral by a one defined over the entire domain Ω but taken in the Cauchy Principal Value sense,

$$\begin{aligned}\triangle\mathbf{L}\int_\Omega \boldsymbol{\Gamma}(\boldsymbol{x},\boldsymbol{x}')\triangle\mathbf{L}\chi(|\boldsymbol{x}-\boldsymbol{x}'|)\langle\boldsymbol{\epsilon}\rangle(\boldsymbol{x}')\,\mathrm{d}\boldsymbol{x}' \approx \underbrace{\left(A_e\triangle\mathbf{L}\int_{r\le r_m}\frac{\mathcal{G}(\boldsymbol{x},\boldsymbol{x}')}{|\boldsymbol{x}-\boldsymbol{x}'|^d}\triangle\mathbf{L}e^{(-|\boldsymbol{x}-\boldsymbol{x}'|/a)}\,\mathrm{d}\boldsymbol{x}'\right)}_{\boldsymbol{L}_{\mathrm{loc}}}\langle\boldsymbol{\epsilon}\rangle(\boldsymbol{x})\\ + A_p r_m^{2\eta}\triangle\mathbf{L}\quad \mathrm{P.V.}\int_\Omega \frac{\mathcal{G}(\boldsymbol{x},\boldsymbol{x}')}{|\boldsymbol{x}-\boldsymbol{x}'|^{d+2\eta}}\triangle\mathbf{L}\langle\boldsymbol{\epsilon}\rangle(\boldsymbol{x}')\,\mathrm{d}\boldsymbol{x}'.\end{aligned} \tag{4.8}$$

The last integral in (4.8) should be taken in the Cauchy Principal Value (P.V.) sense as defined later in (5.7). The expression on the right hand side in (4.8) can be viewed as a sum of the local operator $\boldsymbol{L}_{\mathrm{loc}}$ and the nonlocal operator $\Lambda_{\mathrm{nonloc}}$, acting on the mean strain. These operators are defined as,

$$\begin{aligned}\boldsymbol{L}_{\mathrm{loc}}\langle\boldsymbol{\epsilon}\rangle(\boldsymbol{x}) &= \left(\triangle\mathbf{L}\int_{r\le r_m} A_e\frac{\mathcal{G}(\boldsymbol{x},\boldsymbol{x}')}{|\boldsymbol{x}-\boldsymbol{x}'|^d}e^{(-|\boldsymbol{x}-\boldsymbol{x}'|/a)}\triangle\mathbf{L}\,\mathrm{d}\boldsymbol{x}'\right)\langle\boldsymbol{\epsilon}\rangle(\boldsymbol{x}),\\ \Lambda_{\mathrm{nonloc}}\langle\boldsymbol{\epsilon}\rangle(\boldsymbol{x}) &= A_p r_m^{2\eta}\triangle\mathbf{L}\quad\mathrm{P.V.}\int_\Omega\frac{\mathcal{G}(\boldsymbol{x},\boldsymbol{x}')\triangle\mathbf{L}\langle\boldsymbol{\epsilon}\rangle(\boldsymbol{x}')}{|\boldsymbol{x}-\boldsymbol{x}'|^{d+2\eta}}\,\mathrm{d}\boldsymbol{x}'.\end{aligned} \tag{4.9}$$

The operator $\Lambda_{\mathrm{nonloc}}$ has a power-law kernel and so the integral is interpreted in the principal value sense. Finally, using (3.14) we can express the mean stress via a nonlocal effective modulus operator on the mean strain as,

$$\langle\boldsymbol{\sigma}\rangle = \boldsymbol{L}_*\langle\boldsymbol{\epsilon}\rangle \approx \Big(\langle\boldsymbol{L}\rangle + \boldsymbol{L}_{\mathrm{loc}} + \Lambda_{\mathrm{nonlocal}}\Big)\langle\boldsymbol{\epsilon}\rangle. \tag{4.10}$$

Eq. (4.10) is a second-order small-contrast approximation for the effective modulus valid for the general case of 3D isotropic elasticity.

5. Emergent fractional-derivative operators in effective constitutive law for anti-plane elasticity

Our goal is to further analyze the nonlocal operator $\Lambda_{\mathrm{nonloc}}$ in $(4.9)_2$ to extract the effect of the power-law decay of the nonlocal kernel. During the analysis we will establish a direct correspondence between power-law kernels and fractional Laplacians (along with their derivatives), thereby relating Green's function-type representations (convolutions) and their Fourier symbols. This correspondence will generally serve as a useful mechanics tool for modeling nonlocal properties of materials via fractional derivatives as extensions of local differential operators. In Appendix B, we formally derive this correspondence between the Green's function (and its derivatives) obtained from classical and fractional Laplacian operators, and their Fourier representations.

For simplicity, we demonstrate the results for the case of anti-plane elasticity, so that we are only concerned with the scalar displacement $u(\boldsymbol{x})$, and the strain $\boldsymbol{\epsilon} = \nabla u$ becomes a vector. The elastic tensors of the two phases are taken to be scalar constants, which are the shear moduli of the two phases denoted by μ_1 and μ_2, and their difference is denoted by $\triangle\mu = \mu_1 - \mu_2$. The elastic tensor $\boldsymbol{L}(\boldsymbol{x})$ is now simply the scalar shear modulus $\mu(\boldsymbol{x})$. The problem now is to simply evaluate the expression (4.10) for the case of 3D anti-plane elasticity, with the nonlocal term $\Lambda_{\mathrm{nonloc}}$ being the major focus of the analysis.

Fourier transform convention and interpretation of singular kernels:. Throughout this section, for a function $f(\boldsymbol{x})$, we use the (infinite-space) Fourier transform convention where hats denote the transformed function:[3]

$$\widetilde{f}(\boldsymbol{k}) = \mathcal{F}[f](\boldsymbol{k}) = \int_{\mathbb{R}^3} f(\boldsymbol{x})e^{-i\boldsymbol{k}\cdot\boldsymbol{x}}\,\mathrm{d}\boldsymbol{x}, \qquad f(\boldsymbol{x}) = \mathcal{F}^{-1}[\widetilde{f}](\boldsymbol{x}) = \int_{\mathbb{R}^3}\widetilde{f}(\boldsymbol{k})e^{i\boldsymbol{k}\cdot\boldsymbol{x}}\,\frac{\mathrm{d}\boldsymbol{k}}{(2\pi)^3}.$$

We begin by noting that the Green's function for the reference medium in 3D for anti-plane elasticity is given as,

$$G(r) = A/r, \tag{5.1}$$

where A is a constant related to the reference medium's shear modulus. The operator $\boldsymbol{\Gamma}$ for this reference medium, which is the second derivative of the Green's function, is given by,

$$\Gamma_{ij} = \frac{\partial^2 G}{\partial x_i\partial x_j'} = r^{-3}(-3A\hat{r}_i\hat{r}_j + A\delta_{ij}) = r^{-3}\mathcal{G}_{ij}(\hat{\boldsymbol{r}}), \tag{5.2}$$

where $r_k = x_k - x_k'$ with $\hat{r}_i$ denoting the unit vector, and $\mathcal{G}_{ij}(\hat{\boldsymbol{r}}) = -3A\hat{r}_i\hat{r}_j + A\delta_{ij}$ is a second-order tensor valued function defined on the unit sphere. Using (5.2) in the expression $(4.9)_2$ for the nonlocal operator $\Lambda_{\mathrm{nonloc}}$, and taking the Fourier transform gives,

$$\begin{aligned}\mathcal{F}\big[\Lambda_{\mathrm{nonloc}}\langle\boldsymbol{\epsilon}\rangle(\boldsymbol{x})\big] &\equiv \mathcal{F}\left[A_p r_m^{2\eta}(\triangle\mu)^2\int_{\mathbb{R}^3}\frac{\mathcal{G}_{ij}\langle\epsilon\rangle_j(\boldsymbol{x}')}{r^{3+2\eta}}\,\mathrm{d}\boldsymbol{x}'\right]\\ &= A_p r_m^{2\eta}A(\triangle\mu)^2\Big(-3\mathcal{F}\big[r^{-3-2\eta}\hat{r}_i\hat{r}_j\big] + \mathcal{F}\big[r^{-3-2\eta}\big]\delta_{ij}\Big)\mathcal{F}\big[\langle\epsilon\rangle_j(\boldsymbol{x})\big].\end{aligned} \tag{5.3}$$

[3] In the following, the factor $1/(2\pi)^3$ in the inverse is dropped for notational brevity. When the physical domain Ω is bounded, we extend $\langle\boldsymbol{\epsilon}\rangle(\boldsymbol{x})$ by zero outside Ω so that the Fourier integrals are well-defined (compact support). When $\Omega = \mathbb{R}^3$ is used as an idealization, the Fourier manipulations are interpreted in the standard tempered-distribution sense (equivalently, acting on rapidly decaying test functions / fluctuations); singular integrals with kernels like $|\boldsymbol{x}-\boldsymbol{x}'|^{-3-2\eta}$ are understood in the Cauchy principal value sense.

Here, the integral over Ω is extended to $\mathbb{R}^3$ by noting that $\langle\boldsymbol{\epsilon}\rangle(\boldsymbol{x}) = 0$ outside Ω. The Fourier transforms, $\mathcal{F}\left[r^{-3-2\eta}\hat{r}_i\hat{r}_j\right]$ and $\mathcal{F}\left[r^{-3-2\eta}\right]$, appearing on the right hand side of (5.3) can be related to the Fourier transforms of appropriate fractional Laplacians and their higher-order derivatives, which is now shown below.

A fractional Laplace operator, $(-\Delta)^s$, is a nonlocal integral operator that generalizes the notion of the standard Laplacian to fractional ordered spatial derivatives. More detailed discussion on the standard Laplace equation, fractional Laplace equation, and their Fourier representations and appropriate function spaces is presented in Appendix B, and here we just introduce important concepts that will be needed in our analysis. For $s \in (0,1)$, the positive fractional Laplacian $(-\Delta)^s u(\boldsymbol{x})$, and the negative fractional Laplacian $(-\Delta)^{-s}u(\boldsymbol{x})$ are defined via the integrals as Di Nezza et al. (2012),

$$(-\Delta)^s u(\boldsymbol{x}) = C(d,s)\ \text{P.V.} \int_{\mathbb{R}^d} \frac{u(\boldsymbol{x}) - u(\boldsymbol{x}')}{|\boldsymbol{x}-\boldsymbol{x}'|^{d+2s}}\, \mathrm{d}\boldsymbol{x}', \tag{5.4}$$

$$(-\Delta)^{-s} u(\boldsymbol{x}) = B(d,s) \int_{\mathbb{R}^d} \frac{u(\boldsymbol{x}')}{|\boldsymbol{x}-\boldsymbol{x}'|^{d-2s}}\, \mathrm{d}\boldsymbol{x}', \tag{5.5}$$

where, $C(d,s)$ and $B(d,s)$ are the normalization constants that depend on the dimension d,

$$C(d,s) = \left(\int_{\mathbb{R}^d} \frac{1-\cos z_1}{|\boldsymbol{z}|^{d+2s}}\, \mathrm{d}\boldsymbol{z}\right)^{-1}, \quad B(d,s) = \left(\int_{\mathbb{R}^d} \frac{\cos z_1}{|\boldsymbol{z}|^{d-2s}}\, \mathrm{d}\boldsymbol{z}\right)^{-1}, \tag{5.6}$$

and P.V. denotes the principal value of the integral expressed as the limit,

$$\text{P.V.} \int_{\mathbb{R}^d} \frac{u(\boldsymbol{x}) - u(\boldsymbol{x}')}{|\boldsymbol{x}-\boldsymbol{x}'|^{d+2s}}\, \mathrm{d}\boldsymbol{x}' = \lim_{\epsilon\to 0} \int_{\mathbb{R}^d \setminus B_\epsilon(\boldsymbol{x})} \frac{u(\boldsymbol{x}) - u(\boldsymbol{x}')}{|\boldsymbol{x}-\boldsymbol{x}'|^{d+2s}}\, \mathrm{d}\boldsymbol{x}'. \tag{5.7}$$

The Fourier representation of the fractional Laplace operator in (5.4) is equivalent to a pseudo-differential operator characterized by the symbol $|\boldsymbol{k}|^{2s}$ and is given as,

$$\mathcal{F}[(-\Delta)^s u(\boldsymbol{x})] = |\boldsymbol{k}|^{2s}\mathcal{F}[u(\boldsymbol{x})], \tag{5.8}$$

where $\boldsymbol{k}$ is the transformed variable, and for a negative fractional Laplacian this becomes,

$$\mathcal{F}[(-\Delta)^{-s} u(\boldsymbol{x})] = |\boldsymbol{k}|^{-2s}\mathcal{F}[u(\boldsymbol{x})]. \tag{5.9}$$

One way to generalize the notion of higher-order fractional Laplacians is through their Fourier representation and Green's function representation. Consider a fractional Laplace equation for a positive general fraction $p > 0$ given by,

$$(-\Delta)^p u(\boldsymbol{x}) = f(\boldsymbol{x}), \quad p = m + s, \quad s \in (0,1), \quad m = \lfloor p \rfloor, \tag{5.10}$$

and $u, f \in C_0^\infty(\mathbb{R}^d)$ are smooth functions. The solution $u(\boldsymbol{x})$ can be formally represented by taking the inverse of (5.12) and using Green's function type integral representation,

$$u(\boldsymbol{x}) = (-\Delta)^{-p} f(\boldsymbol{x}) = \int_{\mathbb{R}^d} \frac{B(d,p)}{|\boldsymbol{x}-\boldsymbol{x}'|^{d-2p}} f(\boldsymbol{x}')\, \mathrm{d}\boldsymbol{x}'. \tag{5.11}$$

The corresponding Green's function and its Fourier symbol, denoted by $G^{(p)}$ and $\widetilde{G^{(p)}}$ respectively, can be formally represented as,

$$G^{(p)}(\boldsymbol{x}) = \frac{B(d,p)}{|\boldsymbol{x}|^{d-2p}} \quad \text{and} \quad \widetilde{G^{(p)}}(\boldsymbol{k}) = \mathcal{F}[G^{(p)}(\boldsymbol{x})] = |\boldsymbol{k}|^{-2p}, \tag{5.12}$$

where, $B(d,p)$ is the normalization constant as defined in (5.6).

It can be shown that (see Appendix B.2 for a formal derivation), the Fourier transform of the $2m^{th}$-order partial derivative of the Green's function $G^{(p)}$ can be obtained as:

$$\widetilde{G^{(p)}_{,i_1\cdots i_{2m}}}(\boldsymbol{k}) = \mathcal{F}[G^{(p)}_{,i_1\cdots i_{2m}}(\boldsymbol{x})] = \mathcal{F}[|\boldsymbol{x}|^{-d+2s}\mathcal{G}^{(p)}_{i_1\cdots i_{2m}}(\boldsymbol{x})] = (-1)^m \hat{k}_i \cdots \hat{k}_{i_{2m}} |\boldsymbol{k}|^{-2s} \tag{5.13}$$

where

$$\mathcal{G}^{(p)}_{i_1\cdots i_{2m}}(\boldsymbol{x}) = |\boldsymbol{x}|^{d+2s} G^{(p)}_{,i_1\cdots i_{2m}}(\boldsymbol{x}),$$

is a smooth tensor-valued function on the unit sphere, and the hats denote unit-vectors.

Now for the case $m = 0$, we have $p = s$, and taking the Fourier transform of the second gradient of the Green's function $G^{(s)}$ from (5.12) with $d = 3$, we get,

$$\begin{aligned}\widetilde{G^{(s)}_{,ij}}(\boldsymbol{k}) &= \mathcal{F}[G^{(s)}_{,ij}(\boldsymbol{r})] \\ &= B(d,s)\Big(-(-3+2s)\mathcal{F}[r^{-3-2(1-s)}]\delta_{ij} - (-3+2s)(-5+2s)\mathcal{F}[r^{-3-2(1-s)}\hat{r}_i\hat{r}_j]\Big) \\ &= B(d,s)\Big((1+2\eta)\mathcal{F}[r^{-3-2\eta}]\delta_{ij} - (1+2\eta)(3+2\eta)\mathcal{F}[r^{-3-2\eta}\hat{r}_i\hat{r}_j]\Big).\end{aligned} \tag{5.14}$$

where we have set $\eta = 1 - s$, and as $s \in (0,1)$ so does $\eta \in (0,1)$. Since the derivative operator in real space becomes a polynomial multiplier in the Fourier space, then the Fourier transform of the second gradient of $G^{(s)}$ in (5.12) can also be written as,

$$\widetilde{G^{(s)}_{,ij}}(\boldsymbol{k}) = \mathcal{F}[G^{(s)}_{,ij}(\boldsymbol{r})] = -k_i k_j \mathcal{F}[G^{(s)}] = -k_i k_j |\boldsymbol{k}|^{-2s} = -\hat{k}_i\hat{k}_j|\boldsymbol{k}|^{2\eta}. \tag{5.15}$$

To obtain the Fourier transform of the Laplacian of the Green's function $G^{(s)}$, we simply set $i = j$ or take the trace in Eqs. (5.14)–(5.15) and get,

$$\widetilde{G^{(s)}_{,ii}}(\boldsymbol{k}) = \mathcal{F}[G^{(s)}_{,ii}(\boldsymbol{r})] = B(d,s)\Big(-(1+2\eta)2\eta\mathcal{F}[r^{-3-2\eta}]\Big) = -|\boldsymbol{k}|^{2\eta}. \tag{5.16}$$

Multiplying (5.16) by $1/2\eta$ and adding it to (5.14) we get,

$$\begin{aligned}\widetilde{G^{(s)}_{,ij}}(\boldsymbol{k}) + \frac{1}{2\eta}\widetilde{G^{(s)}_{,kk}}(\boldsymbol{k})\delta_{ij} &= -B(d,s)(1+2\eta)(3+2\eta)\mathcal{F}[r^{-3-2\eta}\hat{r}_i\hat{r}_j] \\ &= -k_ik_j|\boldsymbol{k}|^{-2s} - \frac{1}{2\eta}|\boldsymbol{k}|^{2\eta}\delta_{ij}.\end{aligned} \tag{5.17}$$

Thus, we have expressed the Fourier transform $\mathcal{F}[r^{-3-2\eta}\hat{r}_i\hat{r}_j]$ in terms of the Fourier transforms of the derivatives of the Green's function $\widetilde{G^{(s)}}$. Using (5.17) and (5.16) in (5.3) we get,

$$\begin{aligned}\mathcal{F}\left[\Lambda_{\text{nonloc}}\langle\boldsymbol{\epsilon}\rangle\right]_i &= A_p r_m^{2\eta} A(\triangle\,\mu)^2\Big(-3\mathcal{F}\left[r^{-3-2\eta}\hat{r}_i\hat{r}_j\right] + \mathcal{F}\left[r^{-3-2\eta}\right]\delta_{ij}\Big)\mathcal{F}\left[\langle\epsilon\rangle_j(\boldsymbol{x})\right] \\ &= \frac{A_p r_m^{2\eta} A(\triangle\,\mu)^2}{B(3,s)(1+2\eta)(3+2\eta)}\left[3\left(\widetilde{G^{(1-\eta)}_{,ij}}(\boldsymbol{k}) + \frac{1}{2\eta}\widetilde{G^{(1-\eta)}_{,kk}}(\boldsymbol{k})\delta_{ij}\right) - \frac{3+2\eta}{2\eta}\widetilde{G^{(1-\eta)}_{,kk}}\delta_{ij}\right]\widetilde{\langle\epsilon\rangle}_j(\boldsymbol{k}) \\ &= \frac{A_p r_m^{2\eta} A(\triangle\,\mu)^2}{B(3,s)(1+2\eta)(3+2\eta)}\left[3\big(-k_ik_j|\boldsymbol{k}|^{-2(1-\eta)}\big) + |\boldsymbol{k}|^{2\eta}\delta_{ij}\right]\widetilde{\langle\epsilon\rangle}_j(\boldsymbol{k}).\end{aligned} \tag{5.18}$$

From (5.15), we see that the Fourier symbol $-k_ik_j|\boldsymbol{k}|^{-2(1-\eta)}$ represents the second gradient of the Green's function, $G^{1-\eta}_{,ij}$, which in turn (from (5.5) and (5.12)) characterizes the negative fractional Laplace operator $(-\Delta)^{-(1-\eta)}$. Thus, taking the inverse Fourier transform in (5.18) and using the correspondence between the differential operators and their Fourier space representations we get,

$$\Lambda_{\text{nonloc}}(x,x')\langle\boldsymbol{\epsilon}\rangle(\boldsymbol{x}) = \frac{A_p r_m^{2\eta} A(\triangle\,\mu)^2}{B(3,s)(1+2\eta)(3+2\eta)}\left(3\nabla\nabla(-\Delta)^{-(1-\eta)} + \boldsymbol{I}(-\Delta)^{\eta}\right)\langle\boldsymbol{\epsilon}\rangle(\boldsymbol{x}), \tag{5.19}$$

where $(-\Delta)^{-(1-\eta)}$ is the negative fractional Laplace operator with fractional order $(1-\eta) \in (0,1)$, and $(-\Delta)^{\eta}$ is the fractional Laplace operator with fractional order $\eta \in (0,1)$.

Thus, from (4.10), the effective modulus operator for the case of anti-plane elasticity can be expressed in terms of the fractional Laplacian and the gradients of the negative fractional Laplacian as,

$$\boldsymbol{\mu}_* \approx \underbrace{\langle\mu\rangle\boldsymbol{I} + \boldsymbol{L}_{\text{loc}}}_{\text{Local terms}} + \frac{A_p r_m^{2\eta} A(\triangle\,\mu)^2}{B(3,s)(1+2\eta)(3+2\eta)}\left(3\nabla\nabla(-\Delta)^{-(1-\eta)} + \boldsymbol{I}(-\Delta)^{\eta}\right). \tag{5.20}$$

Here, the effective shear modulus $\boldsymbol{\mu}_*$ is a nonlocal second-order tensor valued operator and is isotropic in the sense that it is equivariant under all rotations. Note that we do not explicitly show the local contributions to the effective modulus as our focus in on the nonlocal terms. The fractional orders $\eta \in (0,1)$ and $1-\eta \in (0,1)$ appearing above in the effective modulus are completely dictated by the composite microstructure through the power-law exponent, 2η, of the autocovariance function $\chi \propto 1/r^{2\eta}$ (see (2.10)).

The results from this section can be extended to the general anisotropic elasticity case where the operator $\boldsymbol{\Gamma}$ will have a more complicated form, but can still be expressed in terms of Green's functions (convolution-type integrals with power-law kernels) and its derivatives obtained as solutions to the standard and fractional Laplace equations.

5.1. Scaling of the nonlocal operator: revealing the fractional size-effect

In (5.20) we have established the nonlocal term as a linear combination of fractional Laplace operators and its derivatives. These nonlocal terms encapsulate all the emergent size-effect, and here we want to extract that effect. Hence, we will analyze only the nonlocal terms in (5.20). In the following analysis, assume for simplicity that the domain $\Omega = \Omega_R$ is a ball $B_R(0) := \{\boldsymbol{x} \in \mathbb{R}^3 : |x| \le R\}$ of radius R centered at the origin. To show the size-effect, we assume the mean strain to be non-zero inside the body and 0 outside,

$$\langle\boldsymbol{\epsilon}\rangle(\boldsymbol{x}) = \begin{cases}\langle\boldsymbol{\epsilon}\rangle(\boldsymbol{x}), & \boldsymbol{x} \in \Omega_R, \\ 0, & \boldsymbol{x} \notin \Omega_R,\end{cases} \tag{5.21}$$

and also assume that the strain is geometrically similar (profile-shape is maintained) as the domain is scaled, as stated in (5.25) below. The mean-stress can be written using (5.20) as,

$$\langle\boldsymbol{\sigma}\rangle = (\text{Local terms})\ \langle\boldsymbol{\epsilon}\rangle + P\ r_m^{2\eta}\ \left(3\nabla\nabla(-\Delta)^{-(1-\eta)} + \boldsymbol{I}(-\Delta)^{\eta}\right)\langle\boldsymbol{\epsilon}\rangle, \tag{5.22}$$

where, the "Local terms" contain the local contributions (size-independent), and the constant $P = \big(A_pA(\triangle\,\mu)^2\big)/(B(3,s)(1+2\eta)(3+2\eta))$ introduced for brevity, depends on the microstructure information.

First, consider only the fractional Laplace operator $(-\Delta)^\eta$ with $\eta \in (0,1)$ acting component-wise on $\langle\boldsymbol{\epsilon}\rangle$, which written in the integral form is (see (5.4)),

$$(-\Delta)^\eta \langle\boldsymbol{\epsilon}\rangle(x) = C(3,\eta)\,\text{P.V.}\int_{\mathbb{R}^3} \frac{\langle\boldsymbol{\epsilon}\rangle(\boldsymbol{x}) - \langle\boldsymbol{\epsilon}\rangle(\boldsymbol{x}')}{|\boldsymbol{x}-\boldsymbol{x}'|^{3+2\eta}}\,\mathrm{d}\boldsymbol{x}'. \tag{5.23}$$

Now we introduce dimensionless variables,

$$\boldsymbol{x} = R\,\boldsymbol{y}, \qquad \boldsymbol{x}' = R\,\boldsymbol{y}', \qquad |\boldsymbol{y}| \le 1, \tag{5.24}$$

so that $\mathrm{d}\boldsymbol{x}' = R^3\,\mathrm{d}\boldsymbol{y}'$. As the strain is geometrically similar, we have

$$\langle\boldsymbol{\epsilon}\rangle(\boldsymbol{x}) = \boldsymbol{E}(\boldsymbol{x}/R) = \boldsymbol{E}(\boldsymbol{y}), \qquad \boldsymbol{x} \in \Omega_R, \tag{5.25}$$

for some fixed reference mean-strain profile $\boldsymbol{E}(\boldsymbol{y})$. Then,

$$\begin{aligned}(-\Delta)^\eta \langle\boldsymbol{\epsilon}\rangle(R\boldsymbol{y}) &= C(3,\eta)\int_{\mathbb{R}^3} \frac{\boldsymbol{E}(\boldsymbol{y}) - \boldsymbol{E}(\boldsymbol{y}')}{|R\boldsymbol{y}-R\boldsymbol{y}'|^{3+2\eta}}R^3\,\mathrm{d}\boldsymbol{y}' \\ &= \frac{C(3,\eta)}{R^{2\eta}}\int_{\mathbb{R}^3} \frac{\boldsymbol{E}(\boldsymbol{y}) - \boldsymbol{E}(\boldsymbol{y}')}{|\boldsymbol{y}-\boldsymbol{y}'|^{3+2\eta}}\,\mathrm{d}\boldsymbol{y}'.\end{aligned} \tag{5.26}$$

The integral in $(5.26)_2$ consists of non-dimensional variables $\boldsymbol{y}$ and $\boldsymbol{y}'$ only, and so we can define the dimensionless function

$$\boldsymbol{F}(\boldsymbol{y}) := C(3,\eta)\int_{\mathbb{R}^3} \frac{\boldsymbol{E}(\boldsymbol{y}) - \boldsymbol{E}(\boldsymbol{y}')}{|\boldsymbol{y}-\boldsymbol{y}'|^{3+2\eta}}\,\mathrm{d}\boldsymbol{y}' = (-\Delta_{\boldsymbol{y}})^\eta \boldsymbol{E}(\boldsymbol{y}). \tag{5.27}$$

Then, for any $\boldsymbol{x} \in \Omega_R$ with $|\boldsymbol{x}| < R$ it follows from (5.26) and (5.27) that,

$$(-\Delta)^\eta \langle\boldsymbol{\epsilon}\rangle(\boldsymbol{x}) = \frac{1}{R^{2\eta}}\boldsymbol{F}\left(\frac{\boldsymbol{x}}{R}\right) = \frac{1}{R^{2\eta}}(-\Delta_{\boldsymbol{y}})^\eta \boldsymbol{E}(\boldsymbol{y}). \tag{5.28}$$

Thus, the fractional Laplacian term scales like $R^{-2\eta}$, with the dependence on position encoded in the dimensionless variable $\boldsymbol{x}/R$.

For the $\nabla\nabla(-\Delta)^{-(1-\eta)}$ term, first consider the inverse fractional Laplace operator $(-\Delta)^{-(1-\eta)}$ acting component-wise on the mean-strain:

$$(-\Delta)^{-(1-\eta)}\langle\boldsymbol{\epsilon}\rangle(\boldsymbol{x}) = B(3,1-\eta)\int_{\mathbb{R}^3} \frac{\langle\boldsymbol{\epsilon}\rangle(\boldsymbol{x}')}{|\boldsymbol{x}-\boldsymbol{x}'|^{1+2\eta}}\,\mathrm{d}\boldsymbol{x}', \tag{5.29}$$

for some constant $B(3,1-\eta)$. Taking the second gradient, we can write

$$\nabla\nabla(-\Delta)^{-(1-\eta)}\langle\boldsymbol{\epsilon}\rangle(\boldsymbol{x}) = \int_{\mathbb{R}^3} \boldsymbol{H}(\boldsymbol{x}-\boldsymbol{x}')\langle\boldsymbol{\epsilon}\rangle(\boldsymbol{x}')\,\mathrm{d}\boldsymbol{x}', \tag{5.30}$$

where $\boldsymbol{H}$ is a matrix-valued kernel. Dimensionally, the negative fractional Laplace operator kernel goes as, $(-\Delta)^{-(1-\eta)} \propto |\boldsymbol{x}-\boldsymbol{x}'|^{-(1+2\eta)}$, and each gradient introduces a factor $\sim |\boldsymbol{x}-\boldsymbol{x}|^{-1}$. Therefore, the kernel $\boldsymbol{H}$ is homogeneous of degree

$$\boldsymbol{H}(\lambda\boldsymbol{r}) = \lambda^{-(3+2\eta)}\boldsymbol{H}(\boldsymbol{r}), \qquad \lambda \in \mathbb{R}, \quad \lambda > 0, \tag{5.31}$$

i.e., $\boldsymbol{H}$ has the same homogeneity exponent as the kernel of $(-\Delta)^\eta$. Knowing this, now we apply (5.30) to the same mean-strain field inside the body as described in (5.25), and again perform a similar non-dimensional analysis by setting $\boldsymbol{x} = R\boldsymbol{y}$ and $\boldsymbol{x}' = R\boldsymbol{y}'$, with $|\boldsymbol{y}| < 1$ which gives,

$$\nabla\nabla(-\Delta)^{-(1-\eta)}\langle\boldsymbol{\epsilon}\rangle(R\boldsymbol{y}) = \int_{\mathbb{R}^3} \boldsymbol{H}(R\boldsymbol{y}-R\boldsymbol{y}')\boldsymbol{E}(\boldsymbol{y}')R^3\,\mathrm{d}\boldsymbol{y}'. \tag{5.32}$$

Using the homogeneity of $\boldsymbol{H}$ we have

$$\nabla\nabla(-\Delta)^{-(1-\eta)}\langle\boldsymbol{\epsilon}\rangle(R\boldsymbol{y}) = \frac{1}{R^{2\eta}}\int_{\mathbb{R}^3} \boldsymbol{H}(\boldsymbol{y}-\boldsymbol{y}')\boldsymbol{E}(\boldsymbol{y}')\,\mathrm{d}\boldsymbol{y}' \tag{5.33}$$

$$= \frac{1}{R^{2\eta}}\boldsymbol{G}(\boldsymbol{y}), \tag{5.34}$$

with the dimensionless function $\boldsymbol{G}(\boldsymbol{y})$ defined as,

$$\boldsymbol{G}(\boldsymbol{y}) := \int_{\mathbb{R}^3} \boldsymbol{H}(\boldsymbol{y}-\boldsymbol{y}')\boldsymbol{E}(\boldsymbol{y}')\,\mathrm{d}\boldsymbol{y}' = \nabla_{\boldsymbol{y}}\nabla_{\boldsymbol{y}}(-\Delta_{\boldsymbol{y}})^{-(1-\eta)}\boldsymbol{E}(\boldsymbol{y}). \tag{5.35}$$

Thus, for any $\boldsymbol{x} \in \Omega_R$ with $|\boldsymbol{x}| < R$ we have the second gradient of the negative fractional Laplace operator, with fractional order $1-\eta$, scaling as $R^{-2\eta}$,

$$\nabla\nabla(-\Delta)^{-(1-\eta)}\langle\boldsymbol{\epsilon}\rangle(\boldsymbol{x}) = \frac{1}{R^{2\eta}}\boldsymbol{G}\left(\frac{\boldsymbol{x}}{R}\right) = \frac{1}{R^{2\eta}}\nabla_{\boldsymbol{y}}\nabla_{\boldsymbol{y}}(-\Delta_{\boldsymbol{y}})^{-(1-\eta)}\boldsymbol{E}(\boldsymbol{y}). \tag{5.36}$$

Using (5.28) and (5.36), the scaling of the nonlocal term Λ_{nonloc} is determined, and the mean-stress from (5.22) is obtained as,

$$\begin{aligned}\langle\boldsymbol{\sigma}\rangle(\boldsymbol{x}) &= (\text{Local terms})\langle\boldsymbol{\epsilon}\rangle + P\frac{r_m^{2\eta}}{R^{2\eta}}\left(3\boldsymbol{G}\left(\frac{\boldsymbol{x}}{R}\right) + \boldsymbol{F}\left(\frac{\boldsymbol{x}}{R}\right)\right), \qquad \forall \boldsymbol{x} \in \Omega_R, \quad \text{or,} \\ \langle\boldsymbol{\sigma}\rangle(R\boldsymbol{y}) &= (\text{Local terms})\boldsymbol{E}(\boldsymbol{y}) + P\frac{r_m^{2\eta}}{R^{2\eta}}\left(3\nabla_{\boldsymbol{y}}\nabla_{\boldsymbol{y}}(-\Delta_{\boldsymbol{y}})^{-(1-\eta)} + \boldsymbol{I}(-\Delta_{\boldsymbol{y}})^\eta\right)\boldsymbol{E}(\boldsymbol{y}).\end{aligned} \tag{5.37}$$

This shows that the mean-stress scales as $R^{-2\eta}$, i.e., a fractional size-effect–dependent on the fractional exponent of the size of the body, while the $\boldsymbol{x}$-dependence is entirely through the dimensionless ratio $\boldsymbol{x}/R$. Note that the functions $\boldsymbol{G}$ and $\boldsymbol{F}$ are dimensionless and do not contribute to the size-effect. Also, it is emphasized that the fractional exponent 2η is directly determined by the microstructure via the autocovariance function $\chi(r)$, which has the power-law exponent 2η.

6. Emergent fractional-derivative operators for 3D isotropic elasticity

We now outline the fractional form of the nonlocal operator in $(4.9)_2$ for the case of three-dimensional static linear isotropic elasticity, i.e., the random heterogeneous medium is made of two isotropic linear elastic phases. So the effective constitutive relation we work with is the same as in (4.10) but now evaluated for the isotropic case. In particular, we will focus on evaluating the nonlocal term $\Lambda_{\text{nonloc}}\langle\boldsymbol{\epsilon}\rangle(\boldsymbol{x})$ for the isotropic case and showing the emergence of fractional derivatives. As in Section 4, we work in the bulk and approximate the Green's function of the reference medium by the infinite-medium Green's tensor. This is consistent with the discussion and assumptions preceding (4.7), where the singular behavior of the kernel is obtained from the infinite-body reference solution.

Let the reference medium be isotropic with Lamé moduli λ_0, μ_0, and let

$$L_{0ijkl} = \lambda_0\,\delta_{ij}\delta_{kl} + \mu_0(\delta_{ik}\delta_{jl} + \delta_{il}\delta_{jk})$$

denote its elasticity tensor. The displacement Green's tensor $G_{im}(\mathbf{r})$, with $\mathbf{r} = \mathbf{x} - \mathbf{x}'$, is the Kelvin solution satisfying

$$L_{0ijkl}\,\partial_j\partial_k G_{lm}(\mathbf{r}) + \delta_{im}\delta(\mathbf{r}) = 0.$$

In $\mathbb{R}^3$, this takes the form

$$G_{im}(\mathbf{r}) = \frac{1}{8\pi\mu_0(\lambda_0+2\mu_0)}\left[(\lambda_0+3\mu_0)\frac{\delta_{im}}{r} + (\lambda_0+\mu_0)\frac{r_i r_m}{r^3}\right], \qquad r = |\mathbf{r}|. \tag{6.1}$$

Equivalently, as concisely stated earlier in (4.5) we can write

$$G_{im}(\mathbf{r}) = \frac{1}{r}\left[A\delta_{im} + B\hat{r}_i\hat{r}_m\right], \quad \hat{r}_i = \frac{r_i}{r}, \quad A = \frac{\lambda_0+3\mu_0}{8\pi\mu(\lambda_0+2\mu_0)}, \quad B = \frac{\lambda_0+\mu_0}{8\pi\mu(\lambda_0+2\mu_0)}, \tag{6.2}$$

where A and B are constants defined in terms of Lame parameters. The symmetrized Green operator acting on strain is then

$$\Gamma_{ijmn}(\mathbf{r}) = \frac{1}{2}\Big(T_{imjn}(\mathbf{r}) + T_{jmin}(\mathbf{r})\Big), \quad T_{imjn}(\mathbf{r}) := \frac{\partial^2 G_{im}}{\partial x_j\,\partial x'_n} \tag{6.3}$$

with

$$\begin{aligned} T_{imjn}(\mathbf{r}) = \frac{1}{r^3}\Big[&A\delta_{im}\delta_{jn} - 3A\delta_{im}\hat{r}_j\hat{r}_n - B(\delta_{ij}\delta_{mn} + \delta_{in}\delta_{mj}) \\ &+ 3B\big(\delta_{ij}\hat{r}_m\hat{r}_n + \delta_{in}\hat{r}_m\hat{r}_j + \delta_{mj}\hat{r}_i\hat{r}_n + \delta_{mn}\hat{r}_i\hat{r}_j + \delta_{jn}\hat{r}_i\hat{r}_m\big) - 15B\hat{r}_i\hat{r}_m\hat{r}_j\hat{r}_n\Big]. \end{aligned} \tag{6.4}$$

Note that $\Gamma_{ijmn}(\mathbf{r}) \sim r^{-3}$, and hence has a singularity of the form r^{-d} in 3D. Consistent with the form in (4.6), we write $\Gamma_{ijmn}(\hat{\boldsymbol{r}}) = \frac{\mathcal{G}_{ijmn}(\boldsymbol{r})}{r^3}$. The elastic contrast $\triangle\,\boldsymbol{L}$ of the two-phase random medium is

$$\triangle\,L_{ijkl} = L^{(1)}_{ijkl} - L^{(2)}_{ijkl} = \triangle\,\lambda\,\delta_{ij}\delta_{kl} + \triangle\,\mu(\delta_{ik}\delta_{jl} + \delta_{il}\delta_{jk}), \tag{6.5}$$

with

$$\triangle\,\lambda = \lambda_1 - \lambda_2, \qquad \triangle\,\mu = \mu_1 - \mu_2.$$

Using (6.5) and (6.3), the nonlocal operator in $(4.9)_2$ can then be written in index notation as

$$\big(\Lambda_{\text{nonloc}}\langle\boldsymbol{\epsilon}\rangle\big)_{ij}(\boldsymbol{x}) = A_p r_m^{2\eta}\,\triangle\,L_{ijab}\quad \text{P.V.}\int_\Omega \frac{\mathcal{G}_{abmn}(\boldsymbol{x},\boldsymbol{x}')\,\triangle\,L_{mnkl}\langle\epsilon\rangle_{kl}(\boldsymbol{x}')}{|\boldsymbol{x}-\boldsymbol{x}'|^{3+2\eta}}\,\mathrm{d}\boldsymbol{x}', \tag{6.6}$$

and further substitution gives (dropping the P.V. notation hereafter),

$$\begin{aligned} \big(\Lambda_{\text{nonloc}}\langle\boldsymbol{\epsilon}\rangle\big)_{ij}(\boldsymbol{x}) = A_p r_m^{2\eta}\bigg(&(\triangle\,\lambda)^2\delta_{ij}\int_\Omega \frac{\mathcal{G}_{aamm}(\boldsymbol{x},\boldsymbol{x}')}{r^{3+2\eta}}\langle\epsilon\rangle_{kk}(\mathbf{x}')\,\mathrm{d}\mathbf{x}' \\ &+ 2\,\triangle\,\lambda\,\triangle\,\mu\int_\Omega \frac{\mathcal{G}_{ijmm}(\boldsymbol{x},\boldsymbol{x}')}{r^{3+2\eta}}\langle\epsilon\rangle_{kk}(\mathbf{x}')\,\mathrm{d}\mathbf{x}' \\ &+ 2\,\triangle\,\lambda\,\triangle\,\mu\delta_{ij}\int_\Omega \frac{\mathcal{G}_{aamn}(\boldsymbol{x},\boldsymbol{x}')}{r^{3+2\eta}}\langle\epsilon\rangle_{mn}(\mathbf{x}')\,\mathrm{d}\mathbf{x}' \\ &+ 4(\triangle\,\mu)^2\int_\Omega \frac{\mathcal{G}_{ijmn}(\boldsymbol{x},\boldsymbol{x}')}{r^{3+2\eta}}\langle\epsilon\rangle_{mn}(\mathbf{x}')\,\mathrm{d}\mathbf{x}'\bigg). \end{aligned} \tag{6.7}$$

Expressions for the fourth-order tensor $\mathcal{G}$ and its contractions appearing in the above equation can be obtained from substituting appropriate indices in (6.4). The term in $(\triangle\lambda)^2$ vanishes as $\mathcal{G}_{aamm}=0$. Also, we have $\mathcal{G}_{ijmm}=(A-B)(\delta_{ij}-3\hat{r}_i\hat{r}_j)$, and $\mathcal{G}_{aamn}=(A-B)(\delta_{mn}-3\hat{r}_m\hat{r}_n)$. Substituting these in (6.7) and taking the Fourier transform, we get

$$
\begin{aligned}
\mathcal{F}\left[\Lambda_{\text{nonloc}}\langle\boldsymbol{\epsilon}\rangle\right]_{ij} &= A_p^{2\eta}\Bigg(2\triangle\lambda\triangle\mu(A-B)\mathcal{F}\left[\frac{\delta_{ij}-3\hat{r}_i\hat{r}_j}{r^{3+2\eta}}\right]\mathcal{F}[\langle\epsilon\rangle_{kk}] \\
&+2\triangle\lambda\triangle\mu\delta_{ij}(A-B)\mathcal{F}\left[\frac{\delta_{mn}-3\hat{r}_m\hat{r}_n}{r^{3+2\eta}}\right]\mathcal{F}[\langle\epsilon\rangle_{mn}] \\
&+4(\triangle\mu)^2\Bigg((A-B)\mathcal{F}\left[\frac{1}{r^{3+2\eta}}\right]\mathcal{F}[\langle\epsilon\rangle_{ij}]+B\mathcal{F}\left[\frac{\delta_{ij}}{r^{3+2\eta}}\right]\mathcal{F}[\langle\epsilon\rangle_{mm}]-3(A-B)\mathcal{F}\left[\frac{\hat{r}_j\hat{r}_n}{r^{3+2\eta}}\right]\mathcal{F}[\langle\epsilon\rangle_{in}] \\
&+6B\mathcal{F}\left[\frac{\hat{r}_i\hat{r}_m}{r^{3+2\eta}}\right]\mathcal{F}[\langle\epsilon\rangle_{jm}]+3B\delta_{ij}\mathcal{F}\left[\frac{\hat{r}_m\hat{r}_n}{r^{3+2\eta}}\right]\mathcal{F}[\langle\epsilon\rangle_{mn}]+3B\mathcal{F}\left[\frac{\hat{r}_i\hat{r}_j}{r^{3+2\eta}}\right]\mathcal{F}[\langle\epsilon\rangle_{mm}] \\
&-15B\mathcal{F}\left[\frac{\hat{r}_i\hat{r}_j\hat{r}_m\hat{r}_n}{r^{3+2\eta}}\right]\mathcal{F}[\langle\epsilon\rangle_{mn}]\Bigg)\Bigg).
\end{aligned}
\tag{6.8}
$$

In (6.8), the Fourier transforms of the strain are multiplied by Fourier transforms of (with a factor of $1/r^{3+2\eta}$) either a constant tensor term, or a term quadratic in $\hat{r}$, or a term quartic in $\hat{r}$ (the last term above). The example in Section 5 (see (5.16) and (5.17)) shows how the Fourier transforms $\mathcal{F}[r^{-3-2\eta}]$ and $\mathcal{F}[r^{-3-2\eta}\hat{r}_i\hat{r}_j]$ can be obtained as a linear combination of the Fourier transforms of the fractional Laplacian of order η and second gradient of the negative fractional Laplacian of order $-(1-\eta)$. Using the same analysis, every term, except the last, in (6.8) can be written as some linear combination of Fourier transforms of positive fractional Laplacian (order η) and second gradient of negative fractional Laplacian (order $-(1-\eta)$) operating on the strain tensor (or its trace). For the last term, we follow the same strategy as in Section 5 and consider the Green's function $G^{(p)}$ of the positive fractional Laplacian of order $p=1+s$, where $s\in(0,1)$ and $\eta=1-s$

$$
G^{(p)}(\boldsymbol{r})=\frac{B(d,p)}{|\boldsymbol{r}|^{d-2p}} \quad \text{and} \quad \widetilde{G^{(p)}}(\boldsymbol{k})=|\boldsymbol{k}|^{-2p}. \tag{6.9}
$$

Also, $G^{(p)}$ is equivalent to the negative fractional Laplacian operator $(-\Delta)^{-p}$ of order $-p$. The Fourier transform of the fourth-order partial derivative of $G^{(p)}$ can then be written as the following linear combination (the exact coefficients are replaced for simplicity with book-keeping coefficients: a_1, a_2, a_3)

$$
\begin{aligned}
\widetilde{G^{(p)}}_{,ijmn}(\boldsymbol{k}) &= a_1\mathcal{F}[\hat{r}_i\hat{r}_j\hat{r}_m\hat{r}_n\ r^{-3-2\eta}]+a_2\delta_{mn}\mathcal{F}[\hat{r}_i\hat{r}_j\ r^{-3-2\eta}]+a_2\delta_{jn}\mathcal{F}[\hat{r}_i\hat{r}_m\ r^{-3-2\eta}] \\
&+a_2\delta_{in}\mathcal{F}[\hat{r}_j\hat{r}_m\ r^{-3-2\eta}]+a_2\delta_{jm}\mathcal{F}[\hat{r}_i\hat{r}_n\ r^{-3-2\eta}]+a_2\delta_{im}\mathcal{F}[\hat{r}_j\hat{r}_n\ r^{-3-2\eta}]+a_2\delta_{ij}\mathcal{F}[\hat{r}_m\hat{r}_n\ r^{-3-2\eta}] \\
&+\big(a_2(\delta_{in}\delta_{jm}+\delta_{jn}\delta_{im})+a_3\delta_{ij}\delta_{mn}\big)\mathcal{F}[r^{-3-2\eta}] \\
&= k_ik_jk_mk_n|\boldsymbol{k}|^{-2-2s}=\hat{k}_i\hat{k}_j\hat{k}_m\hat{k}_n|\boldsymbol{k}|^{2\eta}=\mathcal{F}[\nabla_i\nabla_j\nabla_m\nabla_n(-\Delta)^{-(2-\eta)}]
\end{aligned}
\tag{6.10}
$$

Again the Fourier transforms of the terms quadratic in $\hat{r}$ can be expressed (using the results of Section 5) as some linear combination of $\mathcal{F}[(-\Delta)^{\eta}]$ and $\mathcal{F}[\nabla\nabla(-\Delta)^{-(1-\eta)}]$. Hence, the Fourier transform $\mathcal{F}[\hat{r}_i\hat{r}_j\hat{r}_m\hat{r}_n\ r^{-3-2\eta}]$ can be obtained from (6.10) in terms of the following Fourier transforms (after appropriate tensor products with the identity tensor): $\mathcal{F}[(-\Delta)^{\eta}]$, $\mathcal{F}[\nabla\nabla(-\Delta)^{-(1-\eta)}]$, and $\mathcal{F}[\nabla\nabla\nabla\nabla(-\Delta)^{-(2-\eta)}]$, which can be denoted as,

$$
\mathcal{F}[\hat{r}_i\hat{r}_j\hat{r}_m\hat{r}_n\ r^{-3-2\eta}]=\mathcal{F}[\nabla\nabla\nabla\nabla(-\Delta)^{-(2-\eta)}]_{ijmn}+\big(\text{Lin.Comb.}\{\mathcal{F}[(-\Delta)^{\eta}],\mathcal{F}[\nabla\nabla(-\Delta)^{-(1-\eta)}],\}\big)_{ijmn}. \tag{6.11}
$$

Here, $\text{Lin.Comb.}\{\cdot\}$ is to be interpreted as the linear combination of the bracketed terms after taking appropriate tensor products with the identity tensor.

Now using (6.11) in (6.8) and inverting to real space we can write the nonlocal term as

$$
\begin{aligned}
\left[\Lambda_{\text{nonloc}}\langle\boldsymbol{\epsilon}\rangle\right]_{ij} &= \triangle\lambda\triangle\mu\big(b_1\delta_{ij}(-\Delta)^{\eta}+b_2\nabla_i\nabla_j(-\Delta)^{-(1-\eta)}\big)\langle\epsilon\rangle_{kk} \\
&+\triangle\lambda\triangle\mu\delta_{ij}\big(b_3\delta_{mn}(-\Delta)^{\eta}+b_4\nabla_m\nabla_n(-\Delta)^{-(1-\eta)}\big)\langle\epsilon\rangle_{mn}+(\triangle\mu)^2\Bigg(b_5(-\Delta)^{\eta}\langle\epsilon\rangle_{ij} \\
&+b_6\delta_{ij}(-\Delta)^{\eta}\langle\epsilon\rangle_{mm}+b_7\big(\nabla_j\nabla_n(-\Delta)^{-(1-\eta)}\big)\langle\epsilon\rangle_{in}+b_8\big(\nabla_i\nabla_m(-\Delta)^{-(1-\eta)}\big)\langle\epsilon\rangle_{jm} \\
&+b_9\delta_{ij}\big(\nabla_m\nabla_n(-\Delta)^{-(1-\eta)}\big)\langle\epsilon\rangle_{mn}+b_{10}\big(\nabla_i\nabla_j(-\Delta)^{-(1-\eta)}\big)\langle\epsilon\rangle_{mm} \\
&+b_{11}\big(\nabla_i\nabla_j\nabla_m\nabla_n(-\Delta)^{-(2-\eta)}\big)\langle\epsilon\rangle_{mn}+\big(\text{Lin. Comb}\{\nabla\nabla(-\Delta)^{-(1-\eta)},(-\Delta)^{\eta}\}\big)_{ijmn}\langle\epsilon\rangle_{mn}\Bigg),
\end{aligned}
\tag{6.12}
$$

where $b_1,\ldots,b_{11}$ are constant coefficients that are introduced for brevity (and can be determined exactly). Eq. (6.12) expresses the nonlocal term in terms of fractional Laplacian of order η, second gradient of negative fractional Laplacian of order $-(1-\eta)$, and fourth gradient of negative fractional Laplacian of order $-(2-\eta)$. All the fractional orders are linked directly to the power-law exponent 2η of the covariance function. Finally, this nonlocal term enters the mean stress expression in (4.10) and gives an effective constitutive law expressed using fractional derivatives for an isotropic linear elastic two-phase random medium.

In Appendix B, we characterize the general fractional Laplace operators and show that they can be formally represented by Green's function type convolution operators with power-law kernels and by their equivalent Fourier symbols. This shows that any nonlocal convolution integral with a power-law kernel can be represented as a linear combination of positive and negative fractional Laplace operators and its derivatives. Hence, although this section describes results for 3D isotropic elasticity, the analysis can be extended, with tedious algebra, to the general anisotropic elasticity case.

7. Concluding remarks

In conclusion, this work elucidates the origin of fractional behavior in materials with microstructure by revealing a direct link between the microstructural covariance and the effective fractional order observed in macroscopic models. Our analysis shows that when the autocovariance function of the random composite adheres to a power-law form with a fractional exponent, while satisfying all the necessary constraints on $\chi(r)$, the resulting effective static modulus exhibits a distinct fractional dependence on the size of the material. This finding directly correlates the order of the fractional derivative or integral with the power-law exponent inherent to the microstructural variability.

Our study is based on information extracted from two-point probability functions, offering a fundamental yet robust framework for capturing the essential statistical features of the microstructure. This approach paves the way for explorations in metamaterial design (Florescu et al., 2009; Chen and Torquato, 2018; Wang et al., 2025; Jeulin, 2021), where we can tailor specific micro-geometries and incorporate detailed statistical descriptors to achieve desired fractional and size-dependent effects. It must be noted that several definitions and types of fractional derivatives exist in the literature, which are not all equivalent, and our work uses only a sufficient (rather than necessary) statistical description of the microstructure (the autocovariance function) that leads to the emergent fractional Laplacian operator. The converse may not be true in general. Other mechanisms, such as intrinsic nonlocal interactions at the microscale, the phases themselves being nonlocal, or one of the phases having a sufficiently complex time-history dependence (viscoelastic phase), can also potentially lead to a macroscopic fractional response. If one of the phases by itself is nonlocal, then its response is determined by an intrinsic kernel that also plays a role, and the effective response may have multiple fractional orders or may show a crossover kind of behavior depending on the dominant long-range contribution. These are interesting questions for future work. Also, what is the role or effect of higher-order statistical descriptors (like the 3-point correlation functions) on the fractional behavior is an interesting further question.

Several interesting directions emerge from this work. Future work could potentially build on works on problems pertaining to defects or inclusions, c.f. Bonavia et al. (2025), homogenization and metamaterials (Liu and Reina, 2017, 2018, 2019), architected and templated materials c.f. Grasinger and Dayal (2021), Grasinger (2023), Alizadeh et al. (2004), surface energy-based size-effects (Duan et al., 2005; Wang et al., 2006; He et al., 2025; Mozaffari et al., 2020), electro-magneto-mechanical coupling (Rahmati et al., 2023; Torbati et al., 2022), among others. The existing framework is valid for small-contrast random media, and an interesting future direction we are currently pursuing is to extend the framework to the high-contrast case, which can be applicable, for example, to random media composed of conducting and insulating phases.

A major future direction is extending the framework to dynamics. An effective fractional acoustic wave equation was obtained for a 1D random multiscale medium that showed wave attenuation in a prior work (Garnier and Sølna, 2010). Within the Willis' framework, considering materials with differing phase moduli and phase densities could reveal exotic Willis coupling phenomena c.f. Huynh et al. (2023, 2025). The current work is based on the framework limited to the linear case, and a different framework can be developed to incorporate nonlinearity. We note some interesting progress on the nonlinear analysis of Eshelby's inclusion problem (which is foundational for many homogenization schemes) (Golgoon and Yavari, 2018; Li et al., 2022)

Such extensions may reveal additional fractional calculus features and novel fractional size effects, thereby further enriching our understanding of complex material behaviors and expanding the design possibilities in architecturally engineered materials. The insights gained here open new avenues for tailoring material responses through microstructural engineering, thereby advancing the engineering of complex, nonlocal behaviors across a wide range of applications-from thin-film plasticity to seismic attenuation and the biological sciences.

CRediT authorship contribution statement

Kshiteej J. Deshmukh: Writing – original draft, Methodology, Investigation, Formal analysis; **Liping Liu:** Writing – review & editing, Supervision, Methodology, Investigation, Formal analysis; **Pradeep Sharma:** Writing – review & editing, Supervision, Project administration, Methodology, Investigation, Funding acquisition, Formal analysis, Conceptualization.

Declaration of competing interest

The authors declare that they have no known competing financial interests or personal relationships that could have appeared to influence the work reported in this paper.

Acknowledgments

The authors are extremely grateful for the several helpful discussions and suggestions from researchers within the mechanics community. We would like to thank (in no particular order): Pedro Ponte Castañeda, Arash Yavari, David J. Steigmann, Gal Shmuel, Ken Kamrin, Huiling Duan, Samuel Forest, and Davide Bigoni for their generous help. We would also like to thank the reviewers for their insightful comments, which have significantly improved the paper.

Data availability

No data was used for the research described in the article.

Appendix A. Correlation functions

The n phase random medium is drawn from a sample space $\mathcal{P}(\alpha)$ with some probability measure p, and the specific micro-geometry of any one sample depends on the parameter α. The micro-geometry of a particular realization α, can be modeled by the indicator functions $\mathcal{I}_i(\boldsymbol{x};\alpha)$, where $i = 1,\dots,n$ denotes the phase, and $\mathcal{I}_i(\boldsymbol{x};\alpha) = 1$ if $\boldsymbol{x}$ lies in phase i, otherwise 0. In general, it is impossible to obtain $\mathcal{I}_i(\boldsymbol{x};\alpha)$ for all possible realizations α of the random medium, and for any meaningful analysis we need to use certain "mean" quantities that can be realistically obtained. Here, the mean is the ensemble average taken over possible realizations α.

One such mean quantity is the one-point correlation function, also called as one-point probability function, $S_1^{(i)}(\boldsymbol{x})$ defined for the phase i as,

$$S_1^{(i)}(\boldsymbol{x}) = \langle \mathcal{I}_i(\boldsymbol{x};\alpha)\rangle = \int_{\mathcal{P}(\alpha)} \mathcal{I}_i(\boldsymbol{x};\alpha)p(\,\mathrm{d}\alpha), \tag{A.1}$$

which gives the probability that phase i is at point $\boldsymbol{x}$. Similarly, we can define a 2-point probability function $S_2^{(i)}(\boldsymbol{x}_1,\boldsymbol{x}_2)$, the probability of finding phase i at $\boldsymbol{x}_1$ and $\boldsymbol{x}_2$, given by

$$S_2^{(i)}(\boldsymbol{x}_1,\boldsymbol{x}_2) = \langle \mathcal{I}_i(\boldsymbol{x}_1;\alpha)\mathcal{I}_i(\boldsymbol{x}_2;\alpha)\rangle. \tag{A.2}$$

A random medium is said to be statistically homogeneous if the probability functions do not depend on the absolute positions $\boldsymbol{x}_1,\boldsymbol{x}_2,\dots$, and instead depend only on the relative distances between the points, i.e., they are translation invariant, $S_2^{(i)}(\boldsymbol{x}_1,\boldsymbol{x}_2) = S_2^{(i)}(x_{12})$, where $x_{12} = |\boldsymbol{x}_1 - \boldsymbol{x}_2|$. For statistically homogeneous two-phase media, the one-point probability functions are constant and equal to the volume fraction of the phase, $S_1^{(i)} = \phi_i$.

For a two-phase random medium, the two point probability function for phase 1, can be expressed in terms of the probability functions for the phase 2. Specifically, we have,

$$S_2^{(1)}(\boldsymbol{x}_1,\boldsymbol{x}_2) = 1 - S_1^{(2)}(\boldsymbol{x}_1) - S_1^{(2)}(\boldsymbol{x}_2) + S_1^{(2)}(\boldsymbol{x}_1,\boldsymbol{x}_2), \tag{A.3}$$

and this result can be extended to n-point probability functions as well. The probability that phase 1 is at $\boldsymbol{x}_1$ and phase 2 at $\boldsymbol{x}_2$ can be obtained by writing the 2-point probability function with "dissimilar ends" $S_2^{(12)}(\boldsymbol{x}_1,\boldsymbol{x}_2)$,

$$\begin{aligned} S_2^{(12)}(\boldsymbol{x}_1,\boldsymbol{x}_2) &= \langle \mathcal{I}_1(\boldsymbol{x}_1;\alpha)\mathcal{I}_2(\boldsymbol{x}_2;\alpha)\rangle \\ &= \langle \mathcal{I}_1(\boldsymbol{x}_1;\alpha)(1 - \mathcal{I}_1(\boldsymbol{x}_2;\alpha))\rangle \\ &= S_1^{(1)}(\boldsymbol{x}) - S_2^{(1)}(\boldsymbol{x}_1,\boldsymbol{x}_2) \end{aligned} \tag{A.4}$$

The modulus of the random medium can be expressed using the indicator functions as,

$$\boldsymbol{L}(\boldsymbol{x};\alpha) = \sum_i L_i \mathcal{I}_i(\boldsymbol{x};\alpha), \quad \Longrightarrow \quad \langle \boldsymbol{L}\rangle = \sum_i L_i S_1^{(i)}(\boldsymbol{x}). \tag{A.5}$$

A useful relation for an operator $\boldsymbol{\Gamma}(\boldsymbol{x},\boldsymbol{x}')$ is,

$$\begin{aligned} &\langle \delta\boldsymbol{L}(\boldsymbol{x};\alpha)\boldsymbol{\Gamma}(\boldsymbol{x},\boldsymbol{x}')\delta\boldsymbol{L}(\boldsymbol{x}';\alpha)\rangle \\ &= \langle (\boldsymbol{L}(\boldsymbol{x};\alpha) - \boldsymbol{L}_0)\boldsymbol{\Gamma}(\boldsymbol{x},\boldsymbol{x}')(\boldsymbol{L}(\boldsymbol{x}';\alpha) - \boldsymbol{L}_0)\rangle \\ &= \langle (\boldsymbol{L}(\boldsymbol{x};\alpha)\boldsymbol{\Gamma}(\boldsymbol{x},\boldsymbol{x}')\boldsymbol{L}(\boldsymbol{x}';\alpha)\rangle - \langle \boldsymbol{L}(\boldsymbol{x};\alpha)\boldsymbol{\Gamma}(\boldsymbol{x},\boldsymbol{x}')\boldsymbol{L}_0\rangle - \langle \boldsymbol{L}_0\boldsymbol{\Gamma}(\boldsymbol{x},\boldsymbol{x}')\boldsymbol{L}(\boldsymbol{x}';\alpha)\rangle + \langle \boldsymbol{L}_0\boldsymbol{\Gamma}(\boldsymbol{x},\boldsymbol{x}')\boldsymbol{L}_0\rangle \\ &= \langle (\boldsymbol{L}(\boldsymbol{x};\alpha)\boldsymbol{\Gamma}(\boldsymbol{x},\boldsymbol{x}')\boldsymbol{L}(\boldsymbol{x}';\alpha)\rangle - \boldsymbol{L}_0\boldsymbol{\Gamma}(\boldsymbol{x},\boldsymbol{x}')\boldsymbol{L}_0 - \boldsymbol{L}_0\boldsymbol{\Gamma}(\boldsymbol{x},\boldsymbol{x}')\boldsymbol{L}_0 + \boldsymbol{L}_0\boldsymbol{\Gamma}(\boldsymbol{x},\boldsymbol{x}')\boldsymbol{L}_0 \\ &= \langle (\boldsymbol{L}(\boldsymbol{x};\alpha)\boldsymbol{\Gamma}(\boldsymbol{x},\boldsymbol{x}')\boldsymbol{L}(\boldsymbol{x}';\alpha)\rangle - \langle \boldsymbol{L}\rangle(\boldsymbol{x})\boldsymbol{\Gamma}(\boldsymbol{x},\boldsymbol{x}')\langle \boldsymbol{L}\rangle(\boldsymbol{x}') \quad [\text{Since, } \boldsymbol{L}_0 = \langle \boldsymbol{L}\rangle]. \end{aligned} \tag{A.6}$$

Using (A.2) and (A.5) in the above yields,

$$\begin{aligned} \langle \delta\boldsymbol{L}(\boldsymbol{x};\alpha)\boldsymbol{\Gamma}(\boldsymbol{x},\boldsymbol{x}')\delta\boldsymbol{L}(\boldsymbol{x}';\alpha)\rangle &= \sum_{i,j} L_i\boldsymbol{\Gamma}(\boldsymbol{x},\boldsymbol{x}')L_j S_2^{(ij)}(\boldsymbol{x},\boldsymbol{x}') - \sum_{i,j} L_i\boldsymbol{\Gamma}(\boldsymbol{x},\boldsymbol{x}')L_j S_1^{(i)}(\boldsymbol{x})S_1^{(j)}(\boldsymbol{x}') \\ &= \sum_{i,j} L_i\boldsymbol{\Gamma}(\boldsymbol{x},\boldsymbol{x}')L_j\left(S_2^{(ij)}(\boldsymbol{x},\boldsymbol{x}') - S_1^{(i)}(\boldsymbol{x})S_1^{(j)}(\boldsymbol{x}')\right) \end{aligned} \tag{A.7}$$

For two-phase statistically homogeneous media, the autocovariance $\chi(\boldsymbol{r})$ for phase 1 is defined as,

$$\begin{aligned} \chi(\boldsymbol{r}) &= \langle [\mathcal{I}_1(\boldsymbol{x}) - \phi_1][\mathcal{I}_1(\boldsymbol{x}+\boldsymbol{r}) - \phi_1]\rangle \\ &= \langle \mathcal{I}_1(\boldsymbol{x})\mathcal{I}_1(\boldsymbol{x}+\boldsymbol{r}) - \phi_1\mathcal{I}_1(\boldsymbol{x}) - \phi_1\mathcal{I}_1(\boldsymbol{x}+\boldsymbol{r}) + \phi_1^2]\rangle \\ &= S_2^{(1)}(\boldsymbol{r}) - 2\phi_1^2 + \phi_1^2 \\ \Longrightarrow\ \chi_1(\boldsymbol{r}) &= S_2^{(1)}(\boldsymbol{r}) - \phi_1^2. \end{aligned} \tag{A.8}$$

The autocovariance for phase 1 is the same as the autocovariance for phase 2, and this can be shown by continuing with the above relation as follows

$$\begin{aligned} \chi(\boldsymbol{r}) &= S_2^{(1)}(\boldsymbol{r}) - \phi_1^2 \\ &= 1 - S_1^{(2)}(\boldsymbol{x}) - S_1^{(2)}(\boldsymbol{x}+\boldsymbol{r}) + S_2^{(2)}(\boldsymbol{r}) - \phi_1^2 \\ &= 1 - 2\phi_2 + S_2^{(2)}(\boldsymbol{r}) - (1-\phi_2)^2 \\ \implies \chi(\boldsymbol{r}) &= S_2^{(1)}(\boldsymbol{r}) - \phi_1^2 = S_2^{(2)}(\boldsymbol{r}) - \phi_2^2 \end{aligned} \tag{A.9}$$

For an exhaustive treatment of finding the statistical properties of inhomogeneous random media the reader is referred to the book by Torquato et al. (2002).

Appendix B. Fractional Laplace operators

B.1. Classical Laplace operators

For ease of notation, we consider odd-dimensional space $\mathbb{R}^d$, with $d \geq 3$ and the standard Laplace equation for a source term $f \in C_0(\mathbb{R}^d)$ with compact support (more generally, a tempered distribution):

$$-\Delta u = f. \tag{B.1}$$

Denote the Green's function by

$$G(\boldsymbol{x}) = \frac{\omega_d}{|\boldsymbol{x}|^{d-2}}, \qquad \text{i.e.,} \qquad -\Delta G(\boldsymbol{x}) = \delta(\boldsymbol{x}),$$

and its Fourier transformation by

$$\widetilde{G}(\boldsymbol{k}) = \int_{\mathbb{R}^d} \frac{\omega_d}{|\boldsymbol{x}|^{d-2}} e^{-i\boldsymbol{k}\cdot\boldsymbol{x}} d\boldsymbol{x} \quad \Leftrightarrow \quad G(\boldsymbol{x}) = \int_{\mathbb{R}^d} \widetilde{G}(\boldsymbol{k}) e^{i\boldsymbol{k}\cdot\boldsymbol{x}} \frac{d\boldsymbol{k}}{(2\pi)^d}. \tag{B.2}$$

Here, the constant ω_d is the dimension-dependent normalization constant such that the Green's function satisfies the corresponding Laplace equation. We remark that the two transformation formulas in (B.2) are formal since the integrals are not well-defined *per se*. Its precise interpretation is postponed.

The solution to (B.1) can be written as

$$u(\boldsymbol{x}) = (-\Delta)^{-1} f(\boldsymbol{x}) = \int_{\mathbb{R}^d} G(\boldsymbol{x}-\boldsymbol{y}) f(\boldsymbol{y}) d\boldsymbol{y}. \tag{B.3}$$

The Fourier transformation of (B.1) implies

$$\widetilde{u}(\boldsymbol{k}) = \mathcal{F}[\boldsymbol{u}(\boldsymbol{x})] = \mathcal{F}[(-\Delta)^{-1} f(\boldsymbol{x})] = \frac{\widetilde{f}(\boldsymbol{k})}{|\boldsymbol{k}|^2}. \tag{B.4}$$

Meanwhile, by (B.2)–(B.3) and direct Fourier transformation we also have

$$\begin{aligned} \widetilde{u}(\boldsymbol{k}) &= \int_{\mathbb{R}^d}\int_{\mathbb{R}^d} G(\boldsymbol{x}-\boldsymbol{y}) f(\boldsymbol{y}) e^{-i\boldsymbol{k}\cdot\boldsymbol{x}} d\boldsymbol{y} d\boldsymbol{x} \\ &= \int_{\mathbb{R}^d}\int_{\mathbb{R}^d}\int_{\mathbb{R}^d} \widetilde{G}(\boldsymbol{k}') e^{i\boldsymbol{k}'\cdot(\boldsymbol{x}-\boldsymbol{y})} \frac{d\boldsymbol{k}'}{(2\pi)^d} f(\boldsymbol{y}) e^{-i\boldsymbol{k}\cdot\boldsymbol{x}} d\boldsymbol{y} d\boldsymbol{x} \\ &= \int_{\mathbb{R}^d}\int_{\mathbb{R}^d} \widetilde{G}(\boldsymbol{k}') \int_{\mathbb{R}^d} e^{i(\boldsymbol{k}'-\boldsymbol{k})\cdot\boldsymbol{x}} d\boldsymbol{x} f(\boldsymbol{y}) e^{-i\boldsymbol{k}'\cdot\boldsymbol{y}} \frac{d\boldsymbol{k}'}{(2\pi)^d} d\boldsymbol{y} \\ &= \int_{\mathbb{R}^d}\int_{\mathbb{R}^d} \widetilde{G}(\boldsymbol{k}') \delta(\boldsymbol{k}'-\boldsymbol{k}) f(\boldsymbol{y}) e^{-i\boldsymbol{k}'\cdot\boldsymbol{y}} d\boldsymbol{k}' d\boldsymbol{y} \\ &= \int_{\mathbb{R}^d} \widetilde{G}(\boldsymbol{k}) f(\boldsymbol{y}) e^{-i\boldsymbol{k}\cdot\boldsymbol{y}} d\boldsymbol{y} = \widetilde{G}(\boldsymbol{k}) \widetilde{f}(\boldsymbol{k}). \end{aligned} \tag{B.5}$$

Comparing (B.4) with (B.5), we may identify

$$\widetilde{G}(\boldsymbol{k}) = \frac{1}{|\boldsymbol{k}|^2} = \int_{\mathbb{R}^d} \frac{\omega_d}{|\boldsymbol{x}|^{d-2}} e^{-i\boldsymbol{k}\cdot\boldsymbol{x}} d\boldsymbol{x} = \mathcal{F}[\frac{\omega_d}{|\boldsymbol{x}|^{d-2}}]. \tag{B.6}$$

From this viewpoint, the improperly defined Fourier transformation of the Green's function in (B.6) can be interpreted as a linear transformation such that for any $\widetilde{f} \in C_0^\infty(\mathbb{R}^d)$,

$$\mathcal{F}^{-1}[\widetilde{G}(\boldsymbol{k})\widetilde{f}(\boldsymbol{k})] = (-\Delta)^{-1} f(\boldsymbol{x}). \tag{B.7}$$

Indeed, the formal integral definition of $\widetilde{G}(\boldsymbol{k}) = \mathcal{F}[G(\boldsymbol{x})]$ in (B.6) satisfies that for any $\widetilde{f} \in C_0^\infty(\mathbb{R}^d)$,

$$\mathcal{F}^{-1}[\widetilde{G}(\boldsymbol{k})\widetilde{f}(\boldsymbol{k})] = \int_{\mathbb{R}^d} \widetilde{G}(\boldsymbol{k})\widetilde{f}(\boldsymbol{k}) e^{i\boldsymbol{k}\cdot\boldsymbol{x}} \frac{d\boldsymbol{k}}{(2\pi)^d}$$

$$= \int_{\mathbb{R}^d}\int_{\mathbb{R}^d}\int_{\mathbb{R}^d} \frac{\omega_d}{|\boldsymbol{x}'|^{d-2}} e^{-i\boldsymbol{k}\cdot\boldsymbol{x}'} f(\boldsymbol{y}) e^{-i\boldsymbol{k}\cdot\boldsymbol{y}} e^{i\boldsymbol{k}\cdot\boldsymbol{x}} \frac{d\boldsymbol{k}}{(2\pi)^d} d\boldsymbol{y} d\boldsymbol{x}' \tag{B.8}$$

$$\begin{aligned}
&= \int_{\mathbb{R}^d}\int_{\mathbb{R}^d} \frac{\omega_d}{|\boldsymbol{x}'|^{d-2}} f(\boldsymbol{y})\delta(\boldsymbol{y}+\boldsymbol{x}'-\boldsymbol{x}) d\boldsymbol{y} d\boldsymbol{x}' \\
&= \int_{\mathbb{R}^d} \frac{\omega_d}{|\boldsymbol{x}-\boldsymbol{y}|^{d-2}} f(\boldsymbol{y}) d\boldsymbol{y} \\
&= (-\Delta)^{-1} f(\boldsymbol{x}).
\end{aligned}$$

Moreover, we consider second-order derivatives of $u(\boldsymbol{x})$:

$$u_{,ij}(\boldsymbol{x}) = \int_{\mathbb{R}^d} G_{,ij}(\boldsymbol{x}-\boldsymbol{y}) f(\boldsymbol{y}) d\boldsymbol{y} = \int_{\mathbb{R}^d} |\boldsymbol{x}-\boldsymbol{y}|^{-d} \mathcal{G}^{(1)}_{ij}\Big(\frac{\boldsymbol{x}-\boldsymbol{y}}{|\boldsymbol{x}-\boldsymbol{y}|}\Big) f(\boldsymbol{y}) d\boldsymbol{y}. \tag{B.9}$$

The Fourier transformation of $u_{,ij}(\boldsymbol{x})$ is given by

$$\mathcal{F}[u_{,ij}(\boldsymbol{x})] = -\hat{k}_i\hat{k}_j \widetilde{f}(\boldsymbol{k}) = \mathcal{F}[|\boldsymbol{z}|^{-d}\mathcal{G}^{(1)}_{ij}(\hat{\boldsymbol{z}})](\boldsymbol{k})\widetilde{f}(\boldsymbol{k}).$$

That is,

$$\widetilde{G_{,ij}}(\boldsymbol{k}) = \mathcal{F}[|\boldsymbol{x}|^{-d}\mathcal{G}^{(1)}_{ij}(\hat{\mathbf{x}})] = -\hat{k}_i\hat{k}_j \qquad \Leftrightarrow \qquad \mathcal{F}^{-1}[-\hat{k}_i\hat{k}_j] = G_{,ij}(\boldsymbol{x}). \tag{B.10}$$

Further, we consider p-Laplace equation for some integer $p > 0$:

$$(-\Delta)^p u = f$$

The Green's function is identified as

$$G^{(p)}(\boldsymbol{x}) = \frac{\omega_d^{(p)}}{|\boldsymbol{x}|^{d-2p}}, \qquad \text{i.e.,} \qquad (-\Delta)^p G^{(p)}(\boldsymbol{x}) = \delta(\boldsymbol{x}),$$

and its Fourier transformation by

$$\widetilde{G}^{(p)}(\boldsymbol{k}) = \int_{\mathbb{R}^d} \frac{\omega_d^{(p)}}{|\boldsymbol{x}|^{d-2p}} e^{-i\boldsymbol{k}\cdot\boldsymbol{x}} d\boldsymbol{x} \quad \Leftrightarrow \quad G^{(p)}(\boldsymbol{x}) = \int_{\mathbb{R}^d} \widetilde{G}^{(p)}(\boldsymbol{k}) e^{i\boldsymbol{k}\cdot\boldsymbol{x}} \frac{d\boldsymbol{k}}{(2\pi)^d}. \tag{B.11}$$

Denote $2p$-order derivatives of the Green's function by

$$G^{(p)}_{,i_1i_2\cdots i_{2p}}(\boldsymbol{x}) = \frac{\partial^{2p}}{\partial x_{i_1}\cdots\partial x_{i_{2p}}} G^{(p)}(\boldsymbol{x}) = |\boldsymbol{x}|^{-d}\mathcal{G}^{(p)}_{i_1i_2\cdots i_{2p}}(\hat{\mathbf{x}}) \qquad (\hat{\mathbf{x}} = \frac{\boldsymbol{x}}{|\boldsymbol{x}|}).$$

Analogous to (B.10), we conclude that

$$\begin{aligned}
&\widetilde{G^{(p)}_{,i_1i_2\cdots i_{2p}}}(\boldsymbol{k}) = \mathcal{F}[|\boldsymbol{x}|^{-d}\mathcal{G}^{(p)}_{i_1i_2\cdots i_{2p}}(\hat{\mathbf{x}})] = (-1)^p\hat{k}_{i_1}\hat{k}_{i_2}\cdots\hat{k}_{i_{2p}} \qquad \Longleftrightarrow \\
&\mathcal{F}^{-1}[(-1)^p\hat{k}_{i_1}\hat{k}_{i_2}\cdots\hat{k}_{i_{2p}}] = G^{(p)}_{,i_1i_2\cdots i_{2p}}(\boldsymbol{x}) = |\boldsymbol{x}|^{-d}\mathcal{G}^{(p)}_{i_1i_2\cdots i_{2p}}(\hat{\mathbf{x}}).
\end{aligned} \tag{B.12}$$

B.2. *Fractional Laplace operators*

For $s \in (0,1)$, we interpret the fractional Laplace operators $(-\Delta)^s$ and $(-\Delta)^{-s}$ in terms of fractional convolution with power-law kernels, generalizing the integer-order case. Let $u, f \in C_0^\infty(\mathbb{R}^d)$ be smooth functions with all of its derivatives converging to zero at infinity (more precisely, a tempered distribution). For $s \in (0,1)$, the positive and negative fractional Laplace operators are defined as

$$\begin{aligned}
(-\Delta)^s u(\boldsymbol{x}) &= C(d,s)\text{P.V.}\int_{\mathbb{R}^d} \frac{u(\boldsymbol{x})-u(\boldsymbol{y})}{|\boldsymbol{x}-\boldsymbol{y}|^{d+2s}} d\boldsymbol{y}, \\
(-\Delta)^{-s} f(\boldsymbol{x}) &= B(d,s)\int_{\mathbb{R}^d} \frac{f(\boldsymbol{y})}{|\boldsymbol{x}-\boldsymbol{y}|^{d-2s}} d\boldsymbol{y},
\end{aligned} \tag{B.13}$$

where the principal value and constants $C(d,s)$ and $B(d,s)$ are defined as

$$\begin{aligned}
&\text{P.V.}\int_{\mathbb{R}^d} \frac{u(\boldsymbol{x})-u(\boldsymbol{y})}{|\boldsymbol{x}-\boldsymbol{y}|^{d+2s}} d\boldsymbol{y} = \lim_{\epsilon\to 0}\int_{\mathbb{R}^d\setminus B_\epsilon(x)} \frac{u(\boldsymbol{x})-u(\boldsymbol{y})}{|\boldsymbol{x}-\boldsymbol{y}|^{d+2s}} d\boldsymbol{y}, \\
&C(d,s) = \Big(\int_{\mathbb{R}^d} \frac{1-\cos z_1}{|\boldsymbol{z}|^{d+2s}} d\boldsymbol{z}\Big)^{-1}, \qquad B(d,s) = \Big(\int_{\mathbb{R}^d} \frac{\cos z_1}{|\boldsymbol{z}|^{d-2s}} d\boldsymbol{z}\Big)^{-1}.
\end{aligned} \tag{B.14}$$

Fractional Laplace operators enjoy some neat properties as the usual Laplacian $-\Delta$ or inverse Laplacian $(-\Delta)^{-1}$. In particular, we have

$$\begin{aligned}
&\lim_{s\to 1-}(-\Delta)^s u(\boldsymbol{x}) = -\Delta u(\boldsymbol{x}), \qquad \lim_{s\to 0+}(-\Delta)^s u(\boldsymbol{x}) = u(\boldsymbol{x}), \\
&\lim_{s\to 1-}(-\Delta)^{-s} f(\boldsymbol{x}) = -\Delta^{-1} f(\boldsymbol{x}), \qquad \lim_{s\to 0+}(-\Delta)^{-s} f(\boldsymbol{x}) = f(\boldsymbol{x}).
\end{aligned}$$

We remark that the fractional Laplace operators defined in (B.13) involve nonlocal integral operators with singular kernels of the form $|\boldsymbol{x}-\boldsymbol{y}|^{-d-2s}$ for the positive fractional Laplacian and $|\boldsymbol{x}-\boldsymbol{y}|^{-d+2s}$ for the inverse operator. These kernels generalize the classical Green's function for Laplacian ($G^{(1)}(\boldsymbol{x}) \propto |\boldsymbol{x}|^{-d+2}$). Further, we verify that $\forall\ s \in (0,1)$,

$$\begin{aligned}(-\Delta)^{-s}(-\Delta)^{s}u(\boldsymbol{x}) &= u(\boldsymbol{x}),\\ (-\Delta)^{s}(-\Delta)^{-s}f(\boldsymbol{x}) &= f(\boldsymbol{x}).\end{aligned} \tag{B.15}$$

To see this, we notice that, upon a change of variables $\boldsymbol{y} \to \boldsymbol{z} = \boldsymbol{y}-\boldsymbol{x}$ or $\boldsymbol{y} \to \boldsymbol{z} = \boldsymbol{x}-\boldsymbol{y}$,

$$\int_{\mathbb{R}^d} \frac{u(\boldsymbol{x})-u(\boldsymbol{y})}{|\boldsymbol{x}-\boldsymbol{y}|^{d+2s}} d\boldsymbol{y} = \int_{\mathbb{R}^d} \frac{u(\boldsymbol{x})-u(\boldsymbol{x}+\boldsymbol{z})}{|\boldsymbol{z}|^{d+2s}} d\boldsymbol{z} = \int_{\mathbb{R}^d} \frac{u(\boldsymbol{x})-u(\boldsymbol{x}-\boldsymbol{z})}{|\boldsymbol{z}|^{d+2s}} d\boldsymbol{z}.$$

Therefore, we can alternatively define positive fractional Laplace operators as

$$(-\Delta)^{s}u(\boldsymbol{x}) = -\frac{C(d,s)}{2}\int_{\mathbb{R}^d} \frac{u(\boldsymbol{x}+\boldsymbol{z})+u(\boldsymbol{x}-\boldsymbol{z})-2u(\boldsymbol{x})}{|\boldsymbol{z}|^{d+2s}} d\boldsymbol{z}. \tag{B.16}$$

By Fourier transformation, the above equation implies

$$\begin{aligned}\mathcal{F}[(-\Delta)^{s}u] &= -\frac{C(d,s)}{2}\int_{\mathbb{R}^d} \frac{\mathcal{F}[u(\boldsymbol{x}+\boldsymbol{z})+u(\boldsymbol{x}-\boldsymbol{z})-2u(\boldsymbol{x})]}{|\boldsymbol{z}|^{d+2s}} d\boldsymbol{z}\\ &= C(d,s)\Big[\int_{\mathbb{R}^d} \frac{1-\cos \boldsymbol{k}\cdot\boldsymbol{z}}{|\boldsymbol{z}|^{d+2s}} d\boldsymbol{z}\Big]\mathcal{F}[u]\\ &= |\boldsymbol{k}|^{2s}\mathcal{F}[u].\end{aligned} \tag{B.17}$$

Similarly, we consider Fourier transformation of $(B.13)_2$ and obtain

$$\begin{aligned}\mathcal{F}[(-\Delta)^{-s}f] &= \frac{B(d,s)}{2}\int_{\mathbb{R}^d} \frac{\mathcal{F}[f(\boldsymbol{x}+\boldsymbol{z})+f(\boldsymbol{x}-\boldsymbol{z})]}{|\boldsymbol{z}|^{d-2s}} d\boldsymbol{z}\\ &= B(d,s)\Big[\int_{\mathbb{R}^d} \frac{\cos \boldsymbol{k}\cdot\boldsymbol{z}}{|\boldsymbol{z}|^{d-2s}} d\boldsymbol{z}\Big]\mathcal{F}[f]\\ &= |\boldsymbol{k}|^{-2s}\mathcal{F}[f].\end{aligned} \tag{B.18}$$

By (B.17) and (B.18), we have

$$\mathcal{F}[(-\Delta)^{-s}(-\Delta)^{s}u] = |\boldsymbol{k}|^{-2s}\mathcal{F}[(-\Delta)^{s}u] = \mathcal{F}[u],$$

which completes the proof of (B.15). For $s_1, s_2 > 0$,

$$(-\Delta)^{-s_1}(-\Delta)^{-s_2}u = (-\Delta)^{-(s_1+s_2)}u,$$

since

$$\mathcal{F}[(-\Delta)^{-s_1}(-\Delta)^{-s_2}u] = |\boldsymbol{k}|^{-2s_1}\mathcal{F}[(-\Delta)^{-s_2}u] = |\boldsymbol{k}|^{-2(s_1+s_2)}\mathcal{F}[u]. \tag{B.19}$$

Fractional Laplacian operators are self-adjoint and positive definite in the sense that ($f := (-\Delta)^{s}u$)

$$\begin{aligned}&\int_{\mathbb{R}^d} u(-\Delta)^{s}u = \int_{\mathbb{R}^d} |(-\Delta)^{s/2}u|^2 = \frac{C(d,s)}{2}\int_{\mathbb{R}^d}\int_{\mathbb{R}^d} \frac{|u(\boldsymbol{x})-u(\boldsymbol{y})|^2}{|\boldsymbol{x}-\boldsymbol{y}|^{d+2s}} d\boldsymbol{y}d\boldsymbol{x}\\ &= \int_{\mathbb{R}^d} f(-\Delta)^{-s}f = \int_{\mathbb{R}^d} |(-\Delta)^{-s/2}f|^2 = B(d,s)\int_{\mathbb{R}^d}\int_{\mathbb{R}^d} \frac{f(\boldsymbol{x})f(\boldsymbol{y})}{|\boldsymbol{x}-\boldsymbol{y}|^{d-2s}} d\boldsymbol{y}d\boldsymbol{x}.\end{aligned} \tag{B.20}$$

To see this, by Plancherel's formula we have

$$\begin{aligned}\int_{\mathbb{R}^d} u(-\Delta)^{s}u d\boldsymbol{x} &= C(d,s)\int_{\mathbb{R}^d} u(\boldsymbol{x})\int_{\mathbb{R}^d} \frac{u(\boldsymbol{x})-u(\boldsymbol{y})}{|\boldsymbol{x}-\boldsymbol{y}|^{d+2s}} d\boldsymbol{y}d\boldsymbol{x}\\ &= \int_{\mathbb{R}^d} \mathcal{F}[u]\mathcal{F}[(-\Delta)^{s}u]d\boldsymbol{k} = \int_{\mathbb{R}^d} |\boldsymbol{k}|^{2s}|\mathcal{F}[u]|^2 d\boldsymbol{k}\\ &= \int_{\mathbb{R}^d} \Big||\boldsymbol{k}|^{2\frac{s}{2}}\mathcal{F}[u]\Big|^2 d\boldsymbol{k} = \int_{\mathbb{R}^d} |(-\Delta)^{s/2}u|^2 d\boldsymbol{x},\end{aligned} \tag{B.21}$$

and

$$\begin{aligned}&C(d,s)\int_{\mathbb{R}^d}\int_{\mathbb{R}^d} \frac{|u(\boldsymbol{x})-u(\boldsymbol{y})|^2}{|\boldsymbol{x}-\boldsymbol{y}|^{d+2s}} d\boldsymbol{y}d\boldsymbol{x} = C(d,s)\int_{\mathbb{R}^d}\int_{\mathbb{R}^d} \frac{1}{|\boldsymbol{z}|^{d+2s}}\Big(u(\boldsymbol{z}+\boldsymbol{x})-u(\boldsymbol{x})\Big)^2 d\boldsymbol{x}d\boldsymbol{z}\\ &= C(d,s)\int_{\mathbb{R}^d} \frac{1}{|\boldsymbol{z}|^{d+2s}}\int_{\mathbb{R}^d} \Big(\mathcal{F}[u(\boldsymbol{z}+\boldsymbol{x})-u(\boldsymbol{x})](\boldsymbol{k})\Big)^2 d\boldsymbol{k}d\boldsymbol{z}\\ &= 2C(d,s)\int_{\mathbb{R}^d}\int_{\mathbb{R}^d} \frac{1-\cos \boldsymbol{k}\cdot\boldsymbol{z}}{|\boldsymbol{z}|^{d+2s}}\Big(\mathcal{F}[u]\Big)^2 d\boldsymbol{z}d\boldsymbol{k}\\ &= 2\int_{\mathbb{R}^d} |\boldsymbol{k}|^{2s}\Big(\mathcal{F}[u]\Big)^2 d\boldsymbol{k} = 2\int_{\mathbb{R}^d} |(-\Delta)^{s/2}u|^2 d\boldsymbol{x}.\end{aligned} \tag{B.22}$$

For a general positive fraction $p = m + s$ for some positive integer m and $s \in (0, 1)$, the fractional Laplacian $(-\Delta)^p$ can be defined as

$$(-\Delta)^p u = (-\Delta)^{m+s} u = (-\Delta)^s (-\Delta)^m u = (-\Delta)^m (-\Delta)^s u. \tag{B.23}$$

From the Fourier relation discussed above, we see that the operator $(-\Delta)^p$ is a Fourier multiplier with symbol $|\boldsymbol{k}|^{2p}$:

$$\mathcal{F}[(-\Delta)^p u](\boldsymbol{k}) = |\boldsymbol{k}|^{2p} \mathcal{F}[u](\boldsymbol{k}). \tag{B.24}$$

Also, if $(-\Delta)^p u = f$, the solution u can be formally represented by the Green's function (a fractional power-law kernel):

$$u(\boldsymbol{x}) = (-\Delta)^{-p} f(\boldsymbol{x}) = B(d, p) \int_{\mathbb{R}^d} \frac{f(\boldsymbol{y})}{|\boldsymbol{x} - \boldsymbol{y}|^{d-2p}} d\boldsymbol{y}. \tag{B.25}$$

B.3. Derivatives of fractional Green's functions

We now consider the generalization of the classical results in (B.10) and (B.12) to fractional Laplacians defined by (B.23)–(B.25). Specifically, we aim to characterize the Fourier symbols of derivatives of the fundamental solution $G^{(p)}(\boldsymbol{x})$ to the fractional Laplace equation $(-\Delta)^p u = f$, where $p = m + s,\ s \in (0, 1), m = \lfloor p \rfloor$. The resulting formulas provide a unified perspective on fractional differentiation as a convolution with singular power-law kernels in real space or as a polynomial multiplier operator in Fourier space.

For $p = m + s,\ s \in (0, 1), m = \lfloor p \rfloor$, the Green's function (so that, $(-\Delta)^p G^{(p)}(\boldsymbol{x}) = \delta(\boldsymbol{x})$) and the corresponding Fourier symbol are given by (B.24)–(B.25):

$$G^{(p)}(\boldsymbol{x}) = \frac{B(d, p)}{|\boldsymbol{x}|^{d-2p}} \quad \text{and} \quad \widetilde{G^{(p)}}(\boldsymbol{k}) = \mathcal{F}[G^{(p)}(\boldsymbol{x})] = |\boldsymbol{k}|^{-2p} \tag{B.26}$$

Just as in the integer-order case, we identify the Fourier transformation of the $2m^{th}$-order partial derivatives of the Green's function as:

$$\widetilde{G^{(p)}_{,i_1 \cdots i_{2m}}}(\boldsymbol{k}) = \mathcal{F}[G^{(p)}_{,i_1 \cdots i_{2m}}(\boldsymbol{x})] = \mathcal{F}[|\boldsymbol{x}|^{-d+2s} \mathcal{G}^{(p)}_{i_1 \cdots i_{2m}}(\widetilde{\boldsymbol{x}})] = (-1)^m \hat{k}_i \cdots \hat{k}_{i_{2m}} |\boldsymbol{k}|^{-2s} \tag{B.27}$$

where

$$\mathcal{G}^{(p)}_{i_1 \cdots i_{2m}}(\widetilde{\boldsymbol{x}}) = |\boldsymbol{x}|^{d-2s} G^{(p)}_{,i_1 \cdots i_{2m}}(\boldsymbol{x}),$$

is a smooth tensor-valued function on the unit sphere.

Summary: Operator-Kernel-Fourier symbol Correspondence. $(s \in (0, 1), m \in \mathbb{Z}_{\geq}, p = m + s, *$ – convolution)

Operator	Real Space Operation	Fourier Space multiplier
$(-\Delta)^m$	Local differentiation	$\|\boldsymbol{k}\|^{2m}$
$(-\Delta)^{-m}$	$* \ G^{(m)}(\boldsymbol{x}) \propto \|\boldsymbol{x}\|^{2m-d}$	$\|\boldsymbol{k}\|^{-2m}$
$\nabla^{2m}(-\Delta)^{-m}$	$* \ \|\boldsymbol{x}\|^{-d} \mathcal{G}^{(m)}_{i_1 \cdots i_{2m}}(\hat{\mathbf{x}})$	$\hat{k}_{i_1} \cdots \hat{k}_{i_{2m}}$
$(-\Delta)^s$	$\sim \int \frac{u(\boldsymbol{x})-u(\boldsymbol{y})}{\|\boldsymbol{x}-\boldsymbol{y}\|^{d+2s}} d\boldsymbol{y}$	$\|\boldsymbol{k}\|^{2s}$
$(-\Delta)^{-s}$	$* \ G^{(s)}(\boldsymbol{x}) \propto \|\boldsymbol{x}\|^{2s-d}$	$\|\boldsymbol{k}\|^{-2s}$
$(-\Delta)^p$	$\sim (-\Delta)^m (-\Delta)^s$	$\|\boldsymbol{k}\|^{2p}$
$(-\Delta)^{-p}$	$* \ G^{(p)}(\boldsymbol{x}) \propto \|\boldsymbol{x}\|^{2p-d}$	$\|\boldsymbol{k}\|^{-2p}$
$\nabla^{2m}(-\Delta)^{-p}$	$* \ \|\boldsymbol{x}\|^{-d+2s} \mathcal{G}^{(p)}_{i_1 \cdots i_{2m}}(\hat{\mathbf{x}})$	$(-1)^m \hat{k}_{i_1} \cdots \hat{k}_{i_{2s}} \|\boldsymbol{k}\|^{-2s}$

Conclusion

The power-law kernels appearing in the fractional Laplacian and its inverse are direct generalizations of the classical Green's functions for $-\Delta$, and their Fourier transforms provide consistent extensions of the standard multiplier operators $|\boldsymbol{k}|^{\pm 2m}$ to fractional powers $|\boldsymbol{k}|^{\pm 2p}$. This formal extension establishes relations between fractional Laplacians and their derivatives, convolutions with power-law kernels in real space, and polynomial multipliers in Fourier space. While classical derivatives act locally with integer-power kernels, fractional operators are inherently nonlocal, and their kernels are fractional power-laws. Rigorous justification can be achieved by calculations similar to (B.7)–(B.8) and careful interpretation of improper integrals as in (B.13).

References

Adolfsson, K., Enelund, M., Olsson, P., 2005. On the fractional order model of viscoelasticity. Mech. Time-Depend. Mater. 9, 15–34.

Alizadeh, A., Sharma, P., Ganti, S., LeBoeuf, S.F., Tsakalakos, L., 2004. Templated wide band-gap nanostructures. J. Appl. Phys. 95 (12), 8199–8206.

Ariza, M.P., Conti, S., Ortiz, M., 2024. Fractional strain gradient plasticity and ductile fracture of metals. Eur. J. Mech.-A/Solids 104, 105172.

Bonavia, J.E., Chockalingam, S., Cohen, T., 2025. On the nonlinear eshelby inclusion problem and its isomorphic growth limit. Math. Mech. Solids, 10812865251319798.

Camar-Eddine, M., Milton, G.W., 2005. Non-local interactions in the homogenization closure of thermoelectric functionals. Asymptot. Anal. 41 (3-4), 259–276.

Camar-Eddine, M., Seppecher, P., 2003. Determination of the closure of the set of elasticity functionals. Arch. Ration. Mech. Anal. 170 (3), 211–245.

Castañeda, P.P., Willis, J.R., 1995. The effect of spatial distribution on the effective behavior of composite materials and cracked media. J. Mech. Phys. Solids 43 (12), 1919–1951.
Chen, D., Torquato, S., 2018. Designing disordered hyperuniform two-phase materials with novel physical properties. Acta Mater. 142, 152–161.
Craiem, D., Armentano, R.L., 2007. A fractional derivative model to describe arterial viscoelasticity. Biorheology 44 (4), 251–263.
Dahlberg, C. F.O., Ortiz, M., 2019. Fractional strain-gradient plasticity. Eur. J. Mech.-A/Solids 75, 348–354.
Deshmukh, K., Breitzman, T., Dayal, K., 2022. Multiband homogenization of metamaterials in real-space: higher-order nonlocal models and scattering at external surfaces. J. Mech. Phys. Solids 167, 104992.
Di Nezza, E., Palatucci, G., Valdinoci, E., 2012. Hitchhiker's guide to the fractional sobolev spaces. Bull. Sci. Math. 136 (5), 521–573.
Ding, W., Patnaik, S., Semperlotti, F., 2022. Multiscale nonlocal elasticity: a distributed order fractional formulation. Int. J. Mech. Sci. 226, 107381.
Drapaca, C.S., Sivaloganathan, S., 2012. A fractional model of continuum mechanics. J. Elast. 107 (2), 105–123.
Drugan, W.J., Willis, J.R., 1996. A micromechanics-based nonlocal constitutive equation and estimates of representative volume element size for elastic composites. J. Mech. Phys. Solids 44 (4), 497–524.
Duan, H.L., Wang, J.-x., Huang, Z.P., Karihaloo, B.L., 2005. Size-dependent effective elastic constants of solids containing nano-inhomogeneities with interface stress. J. Mech. Phys. Solids 53 (7), 1574–1596.
Ericksen, J.L., Truesdell, C., 1957. Exact theory of stress and strain in rods and shells. Arch. Ration. Mech. Anal. 1 (1), 295–323.
Eringen, A.C., Edelen, D., 1972. On nonlocal elasticity. Int. J. Eng. Sci. 10 (3), 233–248.
Failla, G., Zingales, M., 2020. Advanced materials modelling via fractional calculus: challenges and perspectives. Philos. Trans. R. Soc. A 378 (2172), 20200050.
Fellah, Z. E.A., Berger, S., Lauriks, W., Depollier, C., 2004. Verification of kramers–kronig relationship in porous materials having a rigid frame. J. Sound Vib. 270 (4-5), 865–885.
Florescu, M., Torquato, S., Steinhardt, P.J., 2009. Designer disordered materials with large, complete photonic band gaps. Proc. Natl. Acad. Sci. 106 (49), 20658–20663.
Forest, S., Sab, K., 1998. Cosserat overall modeling of heterogeneous materials. Mech. Res. Commun. 25 (4), 449–454.
Garnier, J., Sølna, K., 2010. Effective fractional acoustic wave equations in one-dimensional random multiscale media. J. Acoust. Soc. Am. 127 (1), 62–72.
Gemant, A., 1938. XLV. on fractional differentials. Lond. Edinb. Dublin Philos. Mag. J. Sci. 25 (168), 540–549.
Golgoon, A., Yavari, A., 2018. Nonlinear elastic inclusions in anisotropic solids. J. Elast. 130 (2), 239–269.
Grasinger, M., 2023. Polymer networks which locally rotate to accommodate stresses, torques, and deformation. J. Mech. Phys. Solids 175, 105289.
Grasinger, M., Dayal, K., 2021. Architected elastomer networks for optimal electromechanical response. J. Mech. Phys. Solids 146, 104171.
Guo, J., Yin, Y., Peng, G., 2021. Fractional-order viscoelastic model of musculoskeletal tissues: correlation with fractals. Proc. R. Soc. A 477 (2249), 20200990.
He, L., Cheng, G., Zhu, Y., Park, H.S., 2025. Size-dependent strengthening in nanowires: the roles of adatom diffusion and surface curvature on surface dislocation nucleation. Extreme Mech. Lett. 75, 102282.
Huynh, H.D., Nanthakumar, S.S., Park, H.S., Rabczuk, T., Zhuang, X., 2025. The effect of electro-momentum coupling on unidirectional zero reflection in layered generalized willis metamaterials. Extreme Mech. Lett. 77, 102318.
Huynh, H.D., Zhuang, X., Park, H.S., Nanthakumar, S.S., Jin, Y., Rabczuk, T., 2023. Maximizing electro-momentum coupling in generalized 2D willis metamaterials. Extreme Mech. Lett. 61, 101981.
Ionescu, C., Lopes, A., Copot, D., Machado, J.A.T., Bates, J. H.T., 2017. The role of fractional calculus in modeling biological phenomena: a review. Commun. Nonlinear Sci. Numer. Simul. 51, 141–159.
Jeulin, D., 2021. Morphological Models of Random Structures. vol. 447. Springer.
Khandagale, P., Liu, L., Sharma, P., 2024. Statistical mechanics of plasticity: elucidating anomalous size-effects and emergent fractional nonlocal continuum behavior. J. Mech. Phys. Solids 191, 105747.
Kröner, E., 1967. Elasticity theory of materials with long range cohesive forces. Int. J. Solids Struct. 3 (5), 731–742.
Labini, F.S., Vasilyev, N.L., Baryshev, Y.V., 2007. Power law correlations in galaxy distribution and finite volume effects from the sloan digital sky survey data release four. Astron. Astrophys. 465 (1), 23–33.
Laskin, N., 2002. Fractional Schrödinger equation. Phys. Rev. E 66 (5), 056108.
Li, J., Kothari, M., Chockalingam, S., Henzel, T., Zhang, Q., Li, X., Yan, J., Cohen, T., 2022. Nonlinear inclusion theory with application to the growth and morphogenesis of a confined body. J. Mech. Phys. Solids 159, 104709.
Liu, C., Reina, C., 2017. Variational coarse-graining procedure for dynamic homogenization. J. Mech. Phys. Solids 104, 187–206.
Liu, C., Reina, C., 2018. Broadband locally resonant metamaterials with graded hierarchical architecture. J. Appl. Phys. 123 (9), 095108.
Liu, C., Reina, C., 2019. Dynamic homogenization of resonant elastic metamaterials with space/time modulation. Comput. Mech. 64, 147–161.
Luciano, R., Willis, J.R., 2003. Boundary-layer corrections for stress and strain fields in randomly heterogeneous materials. J. Mech. Phys. Solids 51 (6), 1075–1088.
Luciano, R., Willis, J.R., 2005. Fe analysis of stress and strain fields in finite random composite bodies. J. Mech. Phys. Solids 53 (7), 1505–1522.
Magin, R., 2004. Fractional calculus in bioengineering, Part 1. Critical Reviews™ in Biomed. Eng. 32 (1), 1–104.
Magin, R.L., 2010. Fractional calculus models of complex dynamics in biological tissues. Comput. Math. Appl. 59 (5), 1586–1593.
Mashayekhi, S., Hussaini, M.Y., Oates, W., 2019. A physical interpretation of fractional viscoelasticity based on the fractal structure of media: theory and experimental validation. J. Mech. Phys. Solids 128, 137–150.
Mashayekhi, S., Miles, P., Hussaini, M.Y., Oates, W.S., 2018. Fractional viscoelasticity in fractal and non-fractal media: theory, experimental validation, and uncertainty analysis. J. Mech. Phys. Solids 111, 134–156.
Milton, G.W., 2002. The theory of composites. 2002. Cambridge Monographs on Applied and Computational Mathematics, Cambridge University Press. https://doi.org/10.1017/CBO9780511613357
Mindlin, R.D., 1964. Micro-structure in linear elasticity. Arch. Ration. Mech. Anal. 16, 51–78.
Mindlin, R.D., 1965. Second gradient of strain and surface-tension in linear elasticity. Int. J. Solids Struct. 1 (4), 417–438.
Mindlin, R.D., Eshel, N., 1968. On first strain-gradient theories in linear elasticity. Int. J. Solids Struct. 4 (1), 109–124.
Monje, C.A., Chen, Y., Vinagre, B.M., Xue, D., Feliu-Batlle, V., 2010. Fractional-Order Systems and Controls: Fundamentals and Applications. Springer Science & Business Media.
Mori, T., Smith, T.E., Hsu, W.-T., 2020. Common power laws for cities and spatial fractal structures. Proc. Natl. Acad. Sci. 117 (12), 6469–6475.
Mozaffari, K., Yang, S., Sharma, P., 2020. Surface energy and nanoscale mechanics. In: Handbook of Materials Modeling: Applications: Current and Emerging Materials. Springer, pp. 1949–1974.
Mukherjee, A., Jebahi, M., Abatour, M., Forest, S., 2026. Quantitative prediction of size effects using an advanced micromorphic approach. Mech. Mater. 218, 105679.
Nutting, P.G., 1921. A new general law of deformation. J. Frankl. Inst. 191 (5), 679–685.
Oates, W., Stanisaukis, E., Pahari, B.R., Mashayekhi, S., 2021. Entropy dynamics approach to fractional order mechanics with applications to elastomers. In: Behavior and Mechanics of Multifunctional Materials XV. Vol. 11589. SPIE, pp. 23–34.
Pahari, B.R., Oates, W., 2022. Renyi entropy and fractional order mechanics for predicting complex mechanics of materials. In: Behavior and Mechanics of Multifunctional Materials XVI. Vol. 12044. SPIE, pp. 55–63.
Pandey, V., Holm, S., 2016. Linking the fractional derivative and the lomnitz creep law to non-newtonian time-varying viscosity. Phys. Rev. E 94 (3), 032606.
Paradisi, P., Cesari, R., Mainardi, F., Tampieri, F., 2001. The fractional Fick's law for non-local transport processes. Phys. A Stat. Mech. Appl. 293 (1-2), 130–142.
Patnaik, S., Hollkamp, J.P., Semperlotti, F., 2020. Applications of variable-order fractional operators: a review. Proc. R. Soc. A 476 (2234), 20190498.
Patnaik, S., Semperlotti, F., 2020. A generalized fractional-order elastodynamic theory for non-local attenuating media. Proc. R. Soc. A 476 (2238), 20200200.
Ponte Castaneda, P., Willis, J.R., 1988. On the overall properties of nonlinearly viscous composites. Proc. R. Soc. Lond. A. Math. Phys. Sci. 416 (1850), 217–244.
Qin, C., Colwell, L.J., 2018. Power law tails in phylogenetic systems. Proc. Natl. Acad. Sci. 115 (4), 690–695.
Rahmati, A.H., Jia, R., Tan, K., Zhao, X., Deng, Q., Liu, L., Sharma, P., 2023. Theory of hard magnetic soft materials to create magnetoelectricity. J. Mech. Phys. Solids 171, 105136.

Rossikhin, Y.A., Shitikova, M.V., 2009. Application of fractional calculus for dynamic problems of solid mechanics: novel trends and recent results. Appl. Mech. Rev. 63 (1), 010801. https://doi.org/10.1115/1.4000563

Solheim, H., Stanisauskis, E., Miles, P., Oates, W., 2018. Fractional viscoelasticity of soft elastomers and auxetic foams. In: Behavior and Mechanics of Multifunctional Materials and Composites XII. Vol. 10596. SPIE, pp. 11–20.

Stanisauskis, E., Mashayekhi, S., Pahari, B., Mehnert, M., Steinmann, P., Oates, W., 2022. Fractional and fractal order effects in soft elastomers: strain rate and temperature dependent nonlinear mechanics. Mech. Mater. 172, 104390.

Szabo, T.L., 1994. Time domain wave equations for lossy media obeying a frequency power law. J. Acoust. Soc. Am. 96 (1), 491–500.

Torbati, M., Mozaffari, K., Liu, L., Sharma, P., 2022. Coupling of mechanical deformation and electromagnetic fields in biological cells. Rev. Mod. Phys. 94 (2), 025003.

Torquato, S., et al., 2002. Random Heterogeneous Materials: Microstructure and Macroscopic Properties. vol. 16. Springer.

Torvik, P.J., Bagley, R.L., 1984. On the appearance of the fractional derivative in the behavior of real materials. J. Appl. Mech. 51 (2), 294–298.

Toupin, R., 1962. Elastic materials with couple-stresses. Arch. Ration. Mech. Anal. 11 (1), 385–414.

Wang, J., Duan, H.L., Huang, Z.P., Karihaloo, B.L., 2006. A scaling law for properties of nano-structured materials. Proc. R. Soc. A Math. Phys. Eng. Sci. 462 (2069), 1355–1363.

Wang, Y., Guo, J., 2004. Modified Kolsky model for seismic attenuation and dispersion. J. Geophys. Eng. 1 (3), 187–196.

Wang, Y., Qian, Z., Tong, H., Tanaka, H., 2025. Hyperuniform disordered solids with crystal-like stability. Nat. Commun. 16 (1), 1398.

Willis, J.R., 1981a. Variational and related methods for the overall properties of composites. Adv. Appl. Mech. 21, 1–78.

Willis, J.R., 1981b. Variational principles for dynamic problems for inhomogeneous elastic media. Wave Motion 3 (1), 1–11.

Willis, J.R., 1983. The overall elastic response of composite materials. J. Appl. Mech. 50 (4b), 1202–1209. https://doi.org/10.1115/1.3167202

Willis, J.R., 1985. The nonlocal influence of density variations in a composite. Int. J. Solids Struct. 21 (7), 805–817.

Willis, J.R., 2011. Effective constitutive relations for waves in composites and metamaterials. Proc. R. Soc. A Math. Phys. Eng. Sci. 467 (2131), 1865–1879.

Willis, J.R., 2019. From statics of composites to acoustic metamaterials. Philos. Trans. R. Soc. A 377 (2156), 20190099.

Yeong, C. L.Y., Torquato, S., 1998. Reconstructing random media. Phys. Rev. E 57 (1), 495.